

***Arabidopsis* SWC4 binds DNA and recruits the SWR1 complex to modulate histone H2A.Z deposition at key regulatory genes**

Ángeles Gómez-Zambrano^{1,6}, Pedro Crevillén^{1,6}, José M. Franco-Zorrilla², Juan A. López³, Jordi Moreno-Romero⁴, Pawel Roszak⁴, Juan Santos-González⁴, Silvia Jurado¹, Jesús Vázquez⁵, Claudia Köhler⁴, Roberto Solano², Manuel Piñeiro¹ and José A. Jarillo^{1,*}

¹ Centro de Biotecnología y Genómica de Plantas, Universidad Politécnica de Madrid (UPM) - Instituto Nacional de Investigación y Tecnología Agraria y Alimentaria (INIA), Campus Montegancedo UPM, 28223 Pozuelo de Alarcón (Madrid), Spain

² Plant Molecular Genetics Department and Genomics Unit, Centro Nacional de Biotecnología, Consejo Superior de Investigaciones Científicas, 28049 Madrid, Spain.

³ Proteomics Unit. Centro Nacional de Investigaciones Cardiovasculares Carlos III (CNIC), 28029, Madrid, Spain.

⁴ Department of Plant Biology, Uppsala BioCenter, Swedish University of Agricultural Sciences and Linnean Center for Plant Biology, Uppsala, 75652 Sweden.

⁵ Laboratory of Cardiovascular Proteomics, Centro Nacional de Investigaciones Cardiovasculares Carlos III (CNIC), 28029, Madrid, Spain.

⁶ Co-first author

* To whom correspondence should be addressed: jarillo@inia.es

Present address:

Ángeles Gómez-Zambrano: Instituto de Bioquímica Vegetal y Fotosíntesis, Consejo Superior de Investigaciones Científicas and Universidad de Sevilla, 41092, Sevilla, Spain.

Pawel Roszak: The Sainsbury Laboratory, Cambridge, CB2 1LR, UK

Running title: SWC4 modulates histone H2A.Z deposition

Short summary: The *Arabidopsis* homolog of the yeast SANT domain protein Swc4 is a DNA-binding protein that interacts with SWR1 complex subunits. SWC4 regulates plant growth and development through aiding SWR1-C recruitment and modulating H2A.Z deposition at target genes.

ABSTRACT

Deposition of the H2A.Z histone variant by the SWR1 complex (SWR1-C) in regulatory regions of specific loci modulates transcription. Characterization of *Arabidopsis thaliana* mutations in homologs of the yeast SWR1-C has revealed a role for H2A.Z exchange in a variety of developmental processes; nevertheless, the exact composition of the plant SWR1-C and how it is recruited to target genes remains to be established. Here we show that SWC4, the *Arabidopsis* homolog of the yeast SANT domain protein Swc4/Eaf2, is a DNA-binding protein that interacts with SWR1-C subunits. We demonstrate that the *swc4-1* knock-out mutant is embryo lethal, while *SWC4 RNAi* knockdown lines displayed pleiotropic phenotypic alterations in vegetative and reproductive traits, including acceleration of flowering time, indicating that SWC4 controls post-embryonic processes. Transcriptomic analyses and genome-wide profiling of H2A.Z indicate that SWC4 represses transcription of a number of genes including the floral integrator *FT* and key transcription factors mainly by modulating H2A.Z deposition. Interestingly, *SWC4* silencing does not affect H2A.Z deposition in the *FLC* locus nor expression of this gene, a master regulator of flowering previously shown to be controlled by SWR1-C. Importantly, we find that SWC4 is a DNA-binding protein recognizing specific AT-rich DNA elements in chromatin regions of target genes and that *SWC4* silencing impairs SWR1-C binding at *FT*. Collectively, our data suggest that SWC4 regulates plant growth and development through aiding SWR1-C recruitment and modulating H2A.Z deposition.

Key words

Arabidopsis, SWC4, chromatin, SWR1 complex, H2A.Z deposition, flowering time,

INTRODUCTION

The initiation of developmental programs is orchestrated by key transcription factors and chromatin regulators that activate or inhibit target gene expression (Gentry and Hennig, 2014). Chromatin remodeling plays a central role in establishing and maintaining gene expression patterns, and acts through mechanisms such as covalent posttranslational modifications of histones, ATP-dependent nucleosome remodeling and replacement of canonical histones with specialized variants (Ho and Crabtree, 2010; Venkatesh and Workman, 2015).

Histone variants carry modifications from the canonical amino acid sequence and can be exchanged in the same nucleosome at specific locations in the genome (Talbert and Henikoff, 2017). Among histone H2A variants (Kawashima et al., 2015), H2A.Z is the most conserved across eukaryotes (Thatcher and Gorovsky, 1994) and affects multiple biological processes, like regulation of gene expression (Kobor et al., 2004; Mizuguchi et al., 2004), DNA repair (Kalocsay et al., 2009), cell cycle progression (Dhillon et al., 2006) and chromosome stability (Krogan et al., 2004; Rangasamy et al., 2004). In yeast, the SWR1 complex (SWR1-C) contains up to 14 different proteins and mediates the exchange of histone H2A by H2A.Z (Mizuguchi et al., 2004; Nguyen et al., 2013), but how the complex is recruited to its target genes remains largely unknown. H2A.Z is essential for cell viability in metazoans, and possibly in plants (Coleman-Derr and Zilberman, 2012b; Faast et al., 2001; Liu and Gorovsky, 1996; van Daal and Elgin, 1992), and regulates genes that respond to changes in the environment (Kumar and Wigge, 2010; Millar et al., 2006; Sadeghi et al., 2011; Wan et al., 2009). H2A.Z is generally present in the regulatory regions of specific loci and it is believed to generate chromatin regions with particular structural characteristics that favor rapid transcriptional activation (Weber et al., 2014). However, compelling evidence supports that H2A.Z deposition within nucleosomes is also associated with transcriptional silencing (Dai et al., 2017; Guillemette et al., 2005; Marques et al., 2010; Zhang et al., 2005) and the repression at steady state of genes that respond to environmental and developmental stimuli (Coleman-Derr and Zilberman, 2012a; Jarillo and Pineiro,

2015; Smith et al., 2010; Sura et al., 2017). These distinct transcriptional functions of SWR1-C may be explained by its cooperation with other chromatin modifiers, DNA methylation or by post-translational modifications of H2A.Z and other histones, which result in different degrees of nucleosome stability (Billon and Cote, 2012; Coleman-Derr and Zilberman, 2012b; Deal and Henikoff, 2011; Gerhold and Gasser, 2014; Subramanian et al., 2015).

Homologs to most of the yeast SWR1-C subunits have been identified in *Arabidopsis thaliana* (Jarillo and Pineiro, 2015; March-Diaz and Reyes, 2009), suggesting that the SWR1-C may be conserved between yeast and plants. Nevertheless, only four plant SWR1-C subunits like PHOTOPERIOD-INDEPENDENT EARLY FLOWERING 1 (PIE1), ACTIN-RELATED PROTEIN 6 (ARP6), SWR1 COMPLEX 6 (SWC6) and ARP4 have been thoroughly characterized (Choi et al., 2007; Deal et al., 2005; Deal et al., 2007; Lazaro et al., 2008; March-Diaz et al., 2008; Martin-Trillo et al., 2006; Noh and Amasino, 2003). Loss-of function mutations in *PIE1*, *ARP6* or *SWC6* cause misexpression of a number of genes and similar morphological and developmental phenotypic defects affecting vegetative and reproductive traits, including the acceleration of flowering (Choi et al., 2005; Choi et al., 2007; Deal et al., 2005; Deal et al., 2007; Lazaro et al., 2008; March-Diaz and Reyes, 2009; Martin-Trillo et al., 2006). However, although they are part of SWR1-C, these components could have non-redundant functions in plant immunity and gene regulation (Berriri et al., 2016). Silencing of *ARP4* expression also results in strong pleiotropic phenotypic alterations (Kandasamy et al., 2005). Besides, the *Arabidopsis* genome contains three genes encoding H2A.Z variants (Yi et al., 2006), and H2A.Z-deficient (*hta8 hta9 hta11*) mutant plants display developmental phenotypic alterations resembling those present in *swr1-c* mutants (Coleman-Derr and Zilberman, 2012a). Mutations in *SWR1-C* subunit encoding genes also confer hypersensitivity to DNA damaging agents, revealing a pivotal function for the *Arabidopsis* SWR1-C in DNA repair and somatic recombination (Rosa et al., 2013). Moreover, ARP6 regulates different aspects of meiosis (Choi et al., 2013; Qin et al., 2014), and links between H2A.Z

and specification of the origins of DNA replication have been suggested (Costas et al., 2011). A role for the SWR1-C in the fine control of plant development by generating a balance between miRNAs and target mRNAs at the transcriptional level has also recently been unveiled (Choi et al., 2016).

The genetic pathways that regulate *Arabidopsis* flowering time in response to both endogenous and environmental signals converge on a few floral integrator genes such as *FT* and *SUPPRESSOR OF OVEREXPRESSION OF CO1 (SOC1)*. *FLOWERING LOCUS C (FLC)* also has a central role in the control of the floral transition, and acts by repressing the expression of those two floral integrator genes (Andres and Coupland, 2012). In *Arabidopsis*, H2A.Z deposition by SWR1-C is central to regulate flowering time. Mutations in *SWR1-C* genes lead to *FLC* and *MAF4/MAF5* downregulation and early flowering (Jarillo and Pineiro, 2015; Jiang and Berger, 2017). In fact, the transcription start site (TSS) of the *FLC* locus is enriched in H2A.Z, and PIE1 and ARP6 have been shown to be required for the incorporation of this histone variant at *FLC* (Deal et al., 2007). In addition, thermal induction of flowering time is controlled by H2A.Z (Kumar and Wigge, 2010). Under warm temperatures, H2A.Z-containing nucleosomes are lost from regulatory regions in the *FT* promoter, modulating the subsequent accessibility of activating factors such as PHYTOCHROME-INTERACTING FACTOR 4 (PIF4) (Kumar et al., 2012; Kumar and Wigge, 2010). Thus, SWR1-C enables transcriptional plasticity by modulating nucleosome stability and/or the accessibility of regulators to chromatin.

The observations described above and additional experimental evidence support the existence of a plant SWR1-C required to exchange histone H2A by H2A.Z, and that this histone replacement affects gene expression (Deal and Henikoff, 2011). However, in depth functional characterization of most plant SWR1-C subunits still remains elusive. To fill this gap, we identified interacting partners of *Arabidopsis* SWC6 through a proteomics approach. Among others, we found the homolog of the yeast SWR1 complex 4/ Esa1-associated factor 2 (Swc4/Eaf2) and the human DNA methyltransferase-associated protein 1 (DMAP1). We show that the *swc4-1*

knock-out mutant is lethal, revealing the requirement of this gene for *Arabidopsis* embryo development. SWC4 also participates in the regulation of post-embryonic processes, since RNA interference (RNAi) knockdown lines for *SWC4* (*swc4i*) displayed pleiotropic alterations in vegetative and reproductive traits, including acceleration of flowering. Transcriptomic sequencing analyses (RNA-seq) and H2A.Z chromatin immunoprecipitation followed by high-throughput sequencing (ChIP-seq) experiments revealed that SWC4 negatively regulates the expression of the flowering time regulator *FT* and a subset of regulatory key transcription factors by modulating H2A.Z deposition. Intriguingly, we found that SWC4 is able to recognize defined AT-rich DNA elements in TSS-surrounding regions of genes showing upregulated expression and lower levels of H2A.Z in knockdown *swc4i* seedlings. Together, these observations indicate that SWC4 participates in the recruitment of the SWR1-C to target chromatin regions through the recognition of specific AT-rich DNA elements modulating H2A.Z deposition in key regulatory genes.

RESULTS

***Arabidopsis* SWC4 interacts with the core SWR1 complex subunit SWC6**

Arabidopsis SWC6/VPS71 is a HIT-Zn finger-containing protein that is considered a core component of the *Arabidopsis* SWR1-C (Lazaro et al., 2008). To identify novel *Arabidopsis* SWC6 interactors, we initially performed affinity purification followed by tandem mass spectrometry (AP-MS/MS) using a c-Myc tagged SWC6 protein that was previously demonstrated to be fully functional complementing the *swc6* mutation (Lazaro et al., 2008). Proteins co-purified with SWC6-myc in two independent experiments are listed in Supplemental Data S1. The most abundant interactor detected in our proteomics experiments was the well-known SWR1-C subunit ARP6 (Martin-Trillo et al., 2006), confirming previous observations of binding between SWC6 and ARP6 proteins *in vitro* (Lazaro et al., 2008; March-Diaz et al., 2007). We also identified peptides corresponding to other *Arabidopsis* chromatin remodeling complexes including the SWI/SNF ATPase INO80 (Zhang et al., 2015) and ARP8 (Kandasamy et al., 2008) from the INO80 complex, as well as the histone acetyltransferase HAM1 (Latrasse et al., 2008) and AtEAF1 (Bieluszewski et al., 2015) homologs of yeast NuA4 complex (NuA4-C) subunits Esa1 and Eaf1, respectively (Doyon et al., 2004; Lu et al., 2009) (Supplemental Data S1).

In addition to ARP6, we identified other SWR1-C subunits such as PIE1 and SWC2 (Figure 1A), previously shown to interact *in vitro* with SWC6 (Choi et al., 2007; March-Diaz et al., 2007). We also found an *Arabidopsis* YAF9 homolog, YAF9A (Zacharaki et al., 2012), whose interaction with SWC6 was confirmed by yeast two-hybrid (Y2H) analysis (Supplemental Figure S1A). In our experiments, there were also a number of peptides from *Arabidopsis* RVB helicases (Holt et al., 2002) and ARP4 (Kandasamy et al., 2005). However, ARP4 peptides were also present in control samples and ARP4 has been recently reported as a common contaminant in some AP-MS/MS experiments (Van Leene et al., 2015). Besides ARP6, another protein that appeared consistently associated with SWC6 in both experiments was SWC4 (Supplemental Data S1 and Figure 1A). Binding between SWC6 and SWC4

was confirmed by Y2H assays (Figure 1B) and co-immunoprecipitation experiments in *Nicotiana benthamiana* (Figure 1C), corroborating the interaction revealed by the proteomics analysis. SWC4 is one of the subunits shared by SWR1-C and NuA4-C in yeast, together with Yaf9, Arp4 and Actin-1 (Lu et al., 2009). Interestingly, *Arabidopsis* YAF9A also interacts with SWC4 in Y2H experiments (Supplemental Figure S1A), *in vitro* pulldown approaches as shown in Supplemental Figure S1B, and bimolecular fluorescence complementation (BiFC) assays in *N. benthamiana* (Supplemental Figure S1C), corroborating previous observations (Bieluszewski et al., 2015), and suggesting the conservation of the SWC4-YAF9 submodule in plants. Altogether, these results indicate that, as reported in yeast (Kobor et al., 2004), *Arabidopsis* SWC6 co-purified with conserved SWR1-C subunits. To further understand the function of SWR1-C, we undertook a genetic and molecular characterization of the novel *Arabidopsis* SWC4 homolog.

SWC4 is a conserved nuclear protein widely expressed in the plant

Arabidopsis SWC4 is encoded by a single gene, At2g47210, and is homologous to the yeast Swc4/Eaf2 and human DMAP1 proteins (Bittner et al., 2004; Rountree et al., 2000). A phylogenetic analysis confirmed that SWC4 homologs are present in algae, fungi, plants, and metazoans (Supplemental Figure S2A), suggesting an evolutionary conserved role of this protein. Quantitative reverse transcriptase PCR experiments showed that this gene was expressed in all the organs tested, with increased transcript levels detected in proliferating tissues such as roots, flowers, and floral buds (Supplemental Figure S2B). This pattern of expression is consistent with a role of *SWC4* in the regulation of different developmental processes. To determine the subcellular localization of SWC4, a *SWC4-GFP* construct was transiently over-expressed in epidermal cells of *N. benthamiana*. The SWC4-GFP fusion protein was nuclear localized (Supplemental Figure S2C), as expected for a protein that is present in different chromatin remodeling complexes.

SWC4 is essential for male gametophyte function and embryo development

To investigate the role of *Arabidopsis* SWC4 in plant development, we identified *swc4-1*, a knock-out mutant line carrying a T-DNA insertion (Figure 2A). Homozygous *swc4-1* mutants could not be recovered from heterozygous *swc4-1/+* self-pollinated plants, but we were able to maintain the mutation in homozygous condition after complementation with a wild-type SWC4 genomic clone (see METHODS). These data suggested impaired viability of *swc4* mutant embryos or gametophytes. To distinguish between both possibilities, we dissected mature siliques of heterozygous *swc4-1/+* self-pollinated plants. The number of seeds did not differ significantly from Columbia-0 wild-type (WT) plants (Figure 2B); however, there were about 10% of abnormal white seeds that contained embryos arrested at different developmental stages (Figure 2B and 2C), ranging from early torpedo to mature embryos (Figure 2D). White seeds containing mature embryos did not germinate on MS medium, even when the medium was supplemented with gibberellin or the embryos were removed from the silique before desiccation. We speculate that those seeds were homozygous for *swc4-1*. Seeds containing arrested embryos were mainly located close to the stigma (Figure 2E), suggesting that *swc4-1* pollen fails to reach the ovules at the base of the silique. We tested transmission of the *swc4* mutation through male and female gametes by reciprocal crosses of *swc4-1/+* with WT plants. While female transmission was close to the expectation (46 *swc4-1/+* plants among 87 tested), we did not detect *swc4-1/+* mutants when the mutant allele was transmitted through pollen (n=120). Nevertheless, *swc4-1/+* pollen was viable (Supplemental Figure S3A) and formed two sperm cells and one vegetative cell (Supplemental Figure S3B), revealing that the *swc4-1* mutation did not affect pollen development but rather controls post-gametogenesis processes. While we did not detect transmission of *swc4-1* through pollen, the occurrence of abnormal seeds does however suggest that *swc4* mutant pollen can fertilize at low frequency. Together, these results reveal that SWC4 is

required in processes after pollen development and in late stages of embryo development.

RNAi-mediated silencing of *SWC4* expression induces pleiotropic defects in both vegetative and reproductive development.

Because the knockout of *SWC4* resulted in lethality, we generated knockdown lines of *SWC4* by RNAi (Supplemental Figure S4A). These lines displayed phenotypic alterations accompanied by a dramatic reduction in *SWC4* expression levels (Supplemental Figure S4B) compared to WT. Analysis of independent T2 plant lines showed correlation between the severity of the phenotypic alterations and the levels of *SWC4* silencing obtained (Supplemental Figure S4B and S4C). Phenotypic characterization of three representative homozygous *swc4* knockdown lines (432, 712 and 741) rendered similar pleiotropic alterations in both vegetative and reproductive traits (Supplemental Figure S4D). All three RNAi lines display an early flowering phenotype under long days (LD) (Supplemental Figure S4E). On the other hand, overexpression of *SWC4* did not produce any obvious phenotypic alterations (Supplemental Figure S5).

To further explore the post-embryonic function fulfilled by *SWC4*, we performed a detailed phenotypic characterization of the strong *SWC4* RNAi line 712, referred to as *swc4i* in the text hereafter (Figure 2F). Mutations in several *SWR1-C Arabidopsis* homologs cause morphological and developmental abnormalities, including early flowering, curled leaves, and reduced plant size and fertility (Choi et al., 2005; Choi et al., 2007; Deal et al., 2005; Deal et al., 2007; Jarillo and Pineiro, 2015; Lazaro et al., 2008; March-Diaz and Reyes, 2009; Martin-Trillo et al., 2006). Consistently, *swc4i* plants also displayed complex pleiotropic alterations. When grown under either LD and short day (SD) photoperiodic conditions the *swc4i* plants showed reductions in plant size, curled leaves and exhibited symptoms of accelerated leaf senescence (Figure 2G and 2H and Supplemental Figure S4B and S4D). Furthermore, all floral organs and siliques from *swc4i* plants were reduced in

size in comparison to WT (Figure 2I). These observations suggest that SWC4 participates in the regulation of multiple aspects of *Arabidopsis* development.

SWC4 regulates leaf cell proliferation and expansion processes

One of the most striking developmental alterations of *swc4i* plants is their reduced plant and organ size. A reduction in rosette diameter, leaf area, and root length was observed in *swc4i* seedlings (Figure 3A and 3B, and Supplemental Figure S6A and S6B). Smaller plant/organ size may be associated with impaired cellular proliferation and/or cell expansion (Gonzalez et al., 2012). We investigated this by scanning electron microscopy (SEM) to determine the adaxial leaf epidermal cell area and the total number of cells per leaf of *swc4i* plants in comparison to WT (Figure 3C). Analyses of rosette leaves 3 and 4 demonstrated that *swc4i* leaves contained 1.6-fold more adaxial epidermal cells (Figure 3D), whose size was approximately half that of WT epidermal cells (Figure 3E and 3F). The shape of these smaller cells is similar to that of WT epidermal cells.

Cell size is frequently associated with ploidy levels (Meagher et al., 2007). This correlation is apparent for epidermal cell size in leaves and cotyledons (Li et al., 2012). Thus, we carried out a detailed analysis of ploidy levels in mature rosette leaves of *swc4i* and WT 32 day-old plants grown under LD and SD conditions. Flow cytometry measurements of mature leaves 3 and 4 revealed that, compared to WT, *swc4i* displayed an increase of 4C and a reduction of 8C and 16C nuclei levels, which was more evident in plants grown under SD conditions (Figure 3G and 3H). Reduced ploidy levels in *swc4i* plants are consistent with the observed smaller cell size. Altogether, these data indicate that SWC4 activity is required for a proper balance between cell proliferation and expansion.

SWC4 is involved in the regulation of flowering time genes in *Arabidopsis*

Previously identified *Arabidopsis* SWR1-C mutants display an early flowering phenotype (Jarillo and Pineiro, 2015; March-Diaz and Reyes, 2009). We found that *swc4i* plants flowered slightly early under LD conditions when compared to WT plants, but not as early as *swc6-1* (Figure 4A), a representative SWR1-C mutant (Lazaro et al., 2008). However, this flowering time acceleration was not observed under SD conditions. In fact, around 40% of the *swc4i* plants were not able to switch to reproductive development and died, while the remaining ones flowered in a manner similar to WT plants (Figure 4B).

These observations led us to study in detail the expression profile of the floral repressor *FLC* and the floral integrator genes *FT* and *SOC1* in *swc4i* plants. We carried out a time course expression analysis over a 24h period under both LD and SD conditions in 11 and 19 day-old seedlings, respectively (Figure 4C to 4H). The *swc6-1* mutant, whose early flowering phenotype is correlated with decreased *FLC* expression and increased *SOC1* expression levels (Lazaro et al., 2008), was also included in the analysis. Real-time quantitative PCR (Q-PCR) analysis showed that in contrast to the pattern exhibited by the *swc6-1* mutant (Lazaro et al., 2008), *FLC* transcript levels were augmented in *swc4i* under LDs (Figure 4G). Consistently, the expression of the floral integrator gene *SOC1*, normally repressed by *FLC* (Moon et al., 2003), undergoes a reduction in *swc4i* plants under LD conditions (Figure 4E). However, a statistically significant ($p < 0.05$, Student's t-test) increase in the expression of *FT* at the end of the day light period was observed in *swc4i* seedlings (Figure 4C) which may explain the acceleration in flowering time observed in *swc4i* plants under LD conditions (Figure 4A). Remarkably, a peak of *FT* expression at dusk was observed in *swc4i* plants grown under SD conditions (Figure 4D), whereas *SOC1* and *FLC* transcript levels showed similar patterns of expression to WT plants (Figure 4F and 4H). Nevertheless this peak of *FT* under SD conditions expression did not lead to an acceleration of flowering time (Figure 4B), likely because misregulation of other genes may overturn floral transition.

SWC4 depletion results in misregulation of a wide variety of genes

Plants with decreased *SWC4* expression levels displayed several pleiotropic phenotypic alterations, suggesting that this gene participates in the regulation of different developmental processes. To evaluate genes whose expression was misregulated in *swc4i* plants, we performed RNA-seq differential expression analysis and found 1,314 genes upregulated and 395 genes downregulated in *swc4i* seedlings compared to WT (Supplemental Data S2 and Supplemental Figure S7A) using DESeq2 (Love et al., 2014). Interestingly, a number of relevant genes related to the control of the floral transition were differentially expressed, including *FRUITFULL/AGAMOUS-LIKE 8 (FUL/AGL8)* (Gu et al., 1998), *SEPALLATA 3 (SEP3)* (Hwan Lee et al., 2012) and the so called “florigen” gene *FT* (Kardailsky et al., 1999) which appears as one of the most upregulated genes in *swc4i* (Supplemental Data S2).

Singular Enrichment Analysis (SEA) of Gene Ontology (GO) terms of genes that were downregulated in *swc4i* seedlings demonstrated enrichment in biological process categories related to responses to stimulus and stress, and cell death which may be related to the accelerated senescence phenotype observed in *swc4i* plants (Supplemental Figure S7C). Among the upregulated genes, the most significant GO categories enriched were primary and secondary metabolism, and response to stimulus and stress (Supplemental Figure S7B). There were also genes involved in post-embryonic development, cell cycle control, cell differentiation and growth (Supplemental Figure S7B), which may explain the smaller size and cell proliferation defects displayed by *swc4i* plants. All these data are consistent with *SWC4* regulating multiple genes either directly or through a subset of key regulatory genes responsible for its wide role on development.

We compared the transcriptomic profiles of *swc4i* with published RNA-seq data from *pie1*, *arp6*, *swc6*, *h2a.z* double (*hta9 hta11*) and triple (*hta8 hta9 hta11*) mutants (Berriri et al., 2016; Coleman-Derr and Zilberman, 2012a; Kumar and Wigge, 2010; March-Diaz et al., 2008); despite the different plant material and growing conditions used in each experiment, we found a significant overlap in

misregulated genes, that was similar to the level of co-incidence observed among *swr1-c* mutants compared to each other (Supplemental Figure S8 and S9).

SWC4 is involved in H2A.Z deposition

Our proteomic analysis (Figure 1A and Supplemental Data S1) reveals that *Arabidopsis* SWC4 is associated with SWR1-related chromatin remodeling complex. The main role of SWR1-C is to mediate the deposition of the histone variant H2A.Z into the chromatin (Jarillo and Pineiro, 2015). Therefore, we determined the genome-wide distribution of histone H2A.Z in WT and *swc4i* seedlings by ChIP-seq using an antibody against HTA9 (see METHODS and Supplemental Figure S10). Independent biological replicates were highly similar (Supplemental Figure S11-S13) and were therefore analyzed together.

After peak calling, we detected 16,815 and 15,353 H2A.Z genes associated with peaks in WT and *swc4i* plants, respectively (Supplemental Data S3). Peak annotation showed that the H2A.Z signal was strongly enriched towards genic features, with 60% of the peaks localized in gene exons (Figure 5A). Consistent with previous publications (Coleman-Derr and Zilberman, 2012a; Yelagandula et al., 2014), the highest levels of H2A.Z accumulation were detected close to the TSS (Figure 5B and Supplemental Figure S12), with reduced accumulation levels towards gene 3' ends while H2A.Z was depleted in transposon regions (Supplemental Figure S12B,12D,12F and 12H). Heatmap representation of H2A.Z occupancy relative to the TSS in all annotated genes (Figure 5C) corroborated this observation. Comparison between H3 normalized H2A.Z accumulation in Col and *swc4i* revealed decreased H2A.Z levels in *swc4i* seedlings but did not show any strong alteration in the genomic distribution of H2A.Z (Figure 5B and 5C). We performed a statistical analysis of H2A.Z ChIP-enriched regions using SICER (Zang et al., 2009) and identified 5,516 genes with a significant reduction of H2A.Z levels in *swc4i* seedlings compared to WT (FDR <0.01; and Supplemental Data S3). Plotting the H2A.Z signal intensity for all these regions showed a clear

reduction of H2A.Z levels in *swc4i* compared to WT seedling (Figure 5D; * $p < 2.2 \times 10^{-15}$, Wilcoxon rank-sum test).

SEA and GO analysis revealed that H2A.Z-depleted genes in *swc4i* were enriched for a number of biological process categories including DNA metabolism developmental and cellular processes (Supplemental Figure S14A). Interestingly, all the statistically significant functional categories were related to transcriptional regulation and DNA binding activity (Supplemental Figure S14B). We found a statistically significant overlap between upregulated genes and those having reduced levels of H2A.Z (hypergeometric test $p < 0.001$, Figure 5F), while the overlap with downregulated genes was not significant (Figure 5E). Upregulated genes with reduced H2A.Z levels were enriched for genes with DNA binding and control of transcription activities. Among these are 34 transcription factors (Supplemental Data S4) that represent potential targets of SWC4.

***Arabidopsis* SWC4 is a DNA-binding protein that recognizes AT-rich DNA elements**

Arabidopsis SWC4 and all SWC4/DMAP1 homologs bear a conserved DMAP1 C-terminal domain (InterPro IPR008468) (Supplemental Figure S15A) involved in protein-protein interactions (Auger et al., 2008; Bittner et al., 2004; Boyer et al., 2004; Zhou et al., 2010). In addition, SWC4 proteins contain an N-terminal SANT/Myb_DMAP1 domain (InterPro IPR032563; Pfam PF16282) which is related to the SANT (SWI3, ADA2, N-CoR and TFIIB) domain and that has been implicated in the interaction with DNA, histones and other proteins (Aasland et al., 1996; Auger et al., 2008; Boyer et al., 2004; Zhou et al., 2010). The N-terminal SANT domain is essential for yeast survival (Micialkiewicz and Chelstowska, 2008). All SANT domains have structural similarity to the DNA-binding domain of Myb-related proteins (Aasland et al., 1996), with three tandemly repeated α -helices that are arranged in a helix–turn–helix motif (Boyer et al., 2004; Tahirov et al., 2001) (Supplemental Figure S15B). The yeast Adaptor2 (Ada2p) SANT domain

interacts with N-terminal histone tails (Boyer et al., 2002). However, recent evidence indicates that Chd1 chromatin remodeler protein, comprising SANT and SANT-like ISWI domain (SLIDE) domains, may interact with DNA in a non-canonical manner, with preference for AT-rich sequences (Ryan et al., 2011), leading us to hypothesize that the SWC4 SANT/Myb_DMAP1 domain may also bind DNA.

To determine if *Arabidopsis* SWC4 was able to recognize DNA sequences, we performed DNA/protein-binding microarrays (PBMs) (Franco-Zorrilla et al., 2014; Godoy et al., 2011). PBMs result in accurate quantification of protein binding affinities to all possible DNA sequence variations, and it is considered a more comprehensive approach than other *in vitro* methods (Berger and Bulyk, 2009; Godoy et al., 2011). Interestingly, we found that MALTOSE BINDING PROTEIN (MBP)-SWC4 was able to interact with AT-rich elements with great specificity (Z-score value >4.5) and DNA binding affinities as high as those of canonical transcription factors, showing an Enrichment score (E-score) value >0.44 (Figure 6A). No DNA binding at all was observed with MBP protein alone in PBMs experiments. SWC4 DNA-binding capability was corroborated by electrophoretic mobility shift assays (EMSA) showing that SWC4 binds to specific AT-rich elements but not to GC-rich DNA probes (Supplemental Figure S16). All these results indicate that SWC4 is able to specifically recognize a defined set of AT-rich DNA elements (Figure 6A and Supplemental Figure S16).

As a validation of the biological relevance of the PBMs and EMSA experiments, we searched for enrichment of these AT-rich DNA elements in the promoter regions of the most likely SWC4 targets identified in our genomic analyses, those are genes that were upregulated and displayed low H2A.Z levels in *swc4i* plants. AT-rich DNA elements were significantly over-represented within sequences surrounding the TSS of putative SWC4 target genes (hypergeometric test $p < 4.85E-05$), in comparison with the presence of these DNA elements in all *Arabidopsis* genes (Figure 6B). Interestingly, these AT-rich DNA elements were also over-represented around the TSS of the misregulated genes in *arp6-10* (Kumar and Wigge, 2010)

and *h2a.z* triple mutant (Coleman-Derr and Zilberman, 2012a) (Supplemental Figure S17). All these data indicate that SWC4 DNA-binding activity may contribute to the recruitment of SWR1-C to certain genes by recognizing specific AT-rich sequences.

SWC4-mediated H2A.Z deposition regulates *FT* expression

Defects in H2A.Z deposition were previously shown to cause increased *FT* expression (Kumar and Wigge, 2010) and one of the top upregulated genes in *swc4i* plants was the floral regulator *FT* (Supplemental Data S2). However HTA9 signal at *FT* locus is quite low (Kumar et al., 2012) and was not clearly detected in our ChIP-seq. To address whether reduced *SWC4* function promotes chromatin alterations at *FT*, we performed ChIP assays and found that in *swc4i* seedlings HTA9 levels were reduced at *FT* nucleosome +1 (Figure 7A and 7B). Similar results were obtained when an α -HTA9/11 antibody (Zhang et al., 2015) was used (Supplemental Figure S18).

Yeast Swc4 protein is also part of the histone acetyltransferase NuA4-C which is responsible for the acetylation of histone H4 at lysine 5 (H4K5ac) (Doyon and Cote, 2004; Earley et al., 2007). We therefore measured H4K5ac levels at *FT* but we did not detect significant changes of this histone mark in the chromatin regions analyzed in *swc4i* compared to WT seedlings (Figure 7C). All these data show that SWC4 contributes to *FT* gene expression regulation mainly through H2A.Z deposition.

H2A.Z is also required to regulate *FLC* expression (Deal et al., 2007); however we found no difference in *FLC* transcript expression in *swc4i* under SD conditions (Figure 5F), neither relevant changes in H2A.Z nor H4K5ac levels at *FLC* chromatin were observed in *swc4i* compared to WT seedlings (Supplemental Figure S19).

SWC4 binds target loci at AT-rich DNA elements overlapping with H2A.Z peaks

The fact that SWC4 was able to recognize specific AT-rich DNA elements (Figure 6A) prompted us to determine if SWC4 binds them *in vivo*. Using a specific antibody against the full-length *Arabidopsis* SWC4 protein (See METHODS and Supplemental Figure S20), we tested SWC4 binding to the floral regulator *FT*. Q-PCR analysis of the DNA immunoprecipitated with the α -SWC4 antibody from WT seedlings showed that SWC4 binds discrete chromatin locations at the 5' end of the *FT* locus (Figure 7D). Interestingly, SWC4 binding sites overlap with the peak region of H2A.Z present immediately downstream of the TSS of this gene (Figure 7B). To corroborate that SWC4 *in vivo* binding sites colocalize with H2A.Z peaks, we further assessed the binding of SWC4 to the TSS of three key regulatory transcription factors that were upregulated and displayed lower H2A.Z levels in *swc4i* plants, thus representing putative direct targets of SWC4 (Supplemental Data S4): *FUL*, a MADS-domain transcription factor that plays a major role in the development of the *Arabidopsis* fruit and the control of floral transition (Ferrandiz and Fourquin, 2014), *ETHYLENE-RESPONSIVE TRANSCRIPTION FACTOR 9* (*ERF9*), a transcriptional repressor that participates in plant defense mechanisms against necrotic fungi mediated by the ethylene/JA signaling pathway (Maruyama et al., 2013), and *AUXIN-RESPONSIVE PROTEIN 19/MASSUGU2* (*IAA19/MSG2*), a key regulator of auxin response that is required for stress tolerance (Shani et al., 2017). As shown in Figure 8A, SWC4 binding was detected around the TSS of *FUL*, *ERF9*, and *IAA19* genes but not in Ta3 transposon region. Again, the SWC4-binding regions overlap with the H2A.Z peaks detected in our ChIP-seq analysis (Figure 8B).

Consistent with SWC4 binding to defined AT-rich DNA elements *in vitro* (Figure 6), the SWC4-chromatin binding sites determined *in vivo* by ChIP in these genes contain those elements (Figure 8B-8D; Supplemental Data S5). Therefore, SWC4 preferentially binds at regulatory regions of target loci that encompass specific AT-rich elements. In addition, the binding site of this SWR1-C component overlaps with peak regions enriched in H2A.Z in these genes (Figure 7B and Figure 8B-D). Altogether these findings reveal a novel role for SWC4 in the regulation of gene

expression through the recognition of defined AT-rich sequences modulating H2A.Z deposition at target genes by the SWR1-C (Figure 8E). To further test this hypothesis, we sought to investigate whether SWC4 is required for the recruitment of ARP6, a core subunit of the SWR1-C (Martin-Trillo et al., 2006) to the *FT* locus. For this, we carried out ChIP with an anti-ARP6 antibody to explore ARP6 occupancy at *FT* chromatin. In WT, we detected ARP6 binding around the TSS (at positions -38 and +185 from the TSS) (Supplemental Figure S21B and C), coinciding with the enrichment of H2A.Z (Fig. 7). In *swc4i*, ARP6 enrichment at these regions of *FT* was reduced compared with WT (Supplemental Figure S21B and C). These data strongly support a role of SWC4 in recruiting SWR1-C to *FT* chromatin mediating H2A.Z deposition.

DISCUSSION

In this study we have identified the *Arabidopsis* homolog of SWC4/Eaf2/DMAP1 proteins as a novel interactor of SWC6, a core component of the SWR1-C in plants (Lazaro et al., 2008). The identification of other known SWR1-C subunits in our proteomic approach suggests that SWC4 is associated *in vivo* with a conserved plant SWR1-C. Swc4 is also present in the yeast NuA4-C, which mediates the acetylation of histones H4, H2A and H2A.Z (Lu et al., 2009). DMAP1 has been also identified as a component of TIP60 complex in animal cells (Doyon et al., 2004). The *Arabidopsis* genome contains homologs for most of the subunits of the yeast NuA4-C (Jarillo and Pineiro, 2015; March-Diaz and Reyes, 2009), but a functional link between NuA4-C and SWR1-C in plants has not been determined to date. Interestingly, our experiments also revealed an interaction of SWC6 with HAM1 (Supplemental Data S1), a Myst family histone acetyltransferase, considered to be the catalytic subunit of the putative *Arabidopsis* NuA4-C (Latrasse et al., 2008; Xiao et al., 2013). In addition, we found that SWC6 interacts with AtEAF1, a protein proposed as a platform for the putative *Arabidopsis* NuA4-C (Bieluszewski et al., 2015), suggesting that the plant SWR1 and NuA4 complex activities may reside in

a merged TIP60-like complex, as in animals (Billon and Cote, 2012). Further research will be needed to test this hypothesis.

Yeast *Swc4* is an essential gene (Micialkiewicz and Chelstowska, 2008) and *DMAP1* knockout mice embryos abort at preimplantation stage (Mohan et al., 2011). We found that loss of *Arabidopsis SWC4* function caused embryo defects at rather late stages (Figure 2), revealing that loss of *SWC4* has less severe consequences for plant than mammalian embryogenesis. However, the *Arabidopsis swc4-1* mutant largely failed to transmit the mutant allele through the male gametophyte (Figure 2), while gametogenesis was apparently not affected. The described fertility defects of *swc4-1* are stronger than those observed in other *Arabidopsis* SWR1-C mutants that either are viable or display reduced fertility caused by altered anther or ovule development (Kandasamy et al., 2005; Qin et al., 2014; Rosa et al., 2013). A possible explanation for the lethality associated with the *SWC4* loss-of-function mutation may be the concurrent presence of this protein in different chromatin remodeling complexes that are essential for proper embryo development like NuA4-C (Latrasse et al., 2008).

SWC4 knockdown plants show more extreme phenotypic defects than previously characterized SWR1-C mutants. For instance, *swc4i* plants have decreased plant and organ size due to reduced cell size, while *arp6* mutant leaves are composed of fewer total cells rather than a normal number of smaller cells (Deal et al., 2005). Cell size is closely associated with polyploidy in *Arabidopsis* leaves (Meagher et al., 2007). Our results revealed that knocking down *SWC4* expression led to a decrease in the endoreduplication level (Figure 3), suggesting that *SWC4* may participate in the regulation of the entry into endocycle during leaf development. Further analyses will be required to establish the precise role of SWR1-C in leaf maturity programs or in the control of cell cycle regulation in *Arabidopsis*.

Similar to other SWR1-C mutants (March-Diaz and Reyes, 2009) and the *h2a.z* triple mutant (Coleman-Derr and Zilberman, 2012a), *SWC4* knockdown caused accelerated flowering under LD conditions, likely due to *FT* upregulation. However, the early flowering phenotype was not conspicuous under SD conditions, and a

considerable number of *swc4i* plants eventually entered into senescence and died before flowering. We have shown that *swc4i* plants have deregulated expression of about 6% of all protein-coding genes (Supplemental Data S2), with significant overlap with the set of misregulated genes observed in other *swr1-c* mutants and plants depleted in H2A.Z (Supplemental Figure S8 and S9). This list of genes includes a number of candidates that may counteract *FT* upregulation or induce premature plant senescence. In addition, the expression patterns of flowering time genes determined in *swc4i* plants are not totally coincident with those observed in any of the previously characterized SWR1-C mutants, likely indicating the participation of SWC4 in other chromatin-related complexes.

In *Arabidopsis*, H2A.Z occupancy at nucleosome +1 inversely correlates with gene expression (Dai et al., 2017), suggesting that this histone variant might be evicted during transcription (Talbert and Henikoff, 2017). However, the presence of H2A.Z at +1 nucleosome in certain genes is required for maintenance of transcriptional activity (Cai et al., 2017; Deal et al., 2007; Sura et al., 2017). Thus, H2A.Z located at TSS proximal regions is not exclusively involved in promoting transcription (Weber and Henikoff, 2014), but may rather configure the chromatin structure to modulate proper gene expression in response to cellular or environmental cues (Subramanian et al., 2015). A number of results indicate that *Arabidopsis* SWC4 may contribute to regulation of gene expression through modulation of H2A.Z dynamics. In agreement with the pleiotropic phenotypic alterations displayed by the *swc4i* lines, we found nearly 1,800 misregulated genes in these plants, with more than three times as many genes upregulated than downregulated. In addition, SWC4 depletion reduces H2A.Z levels in more than 5,000 genes including a significant overlap with genes upregulated in *swc4i* (Figure 5F). Thus, these data suggest that *Arabidopsis* SWC4 has a major function in transcriptional repression as proposed earlier for other *Arabidopsis* SWR1-C components (Coleman-Derr and Zilberman, 2012a; Dai et al., 2017; Smith et al., 2010) or for the SWR1-C in other species (Guillemette et al., 2005; Marques et al., 2010; Zhang et al., 2005).

In all eukaryotes analyzed, nucleosome-free DNA regions (NFR) are marked by H2A.Z-containing nucleosomes around the TSS (Mavrigh et al., 2008; Raisner et al., 2005; Zilberman et al., 2008). Although SWR1-C is known to catalyze ATP-dependent deposition of H2A.Z (Jarillo and Pineiro, 2015), the recruitment mechanism of SWR1-C to specific genomic regions remains unclear. Swc4 is part of the N-module which plays a critical role in facilitating the contact of SWR1-C with the nucleosome (Gerhold and Gasser, 2014; Kapoor and Shen, 2014). In addition, yeast Swc4 can be detected associated to nucleosomes independently of SWR1-C (Yen et al., 2013). All SWC4 homologs are characterized by bearing a SANT/Myb_DMAP1 domain which is structurally related to Myb-like DNA binding domains. In fact, recent evidence indicates that a protein harboring SANT and SLIDE domains may interact with AT-rich sequences (Ryan et al., 2011). Consistent with this observation, we found that *Arabidopsis* SWC4 is able to bind AT-rich DNA sequences with high affinity. These AT-rich DNA elements are over-represented in the promoter sequences of upregulated genes with lower H2A.Z levels in *SWC4* knockdown plants, and around the TSS of the misregulated genes in *arp6-10* and *h2a.z* triple mutant (Supplemental Figure S17), indicating that SWC4 DNA-binding activity may contribute to the recruitment of SWR1-C to certain target genes recognizing specific AT-rich sequences.

Consistent with the role of SWC4 on H2A.Z dynamics, we found that SWC4 protein *in vivo* binds to the *FT* locus and other key developmental regulators such as *FUL*, *ERF9* and *IAA19* at H2A.Z-enriched regions around nucleosome +1 containing specific SWC4 AT-rich DNA binding elements (Figure 7 and 8). These genes are derepressed and show reduced H2A.Z levels in *SWC4* knockdown plants. *FT*, one of the most upregulated genes in our transcriptomic analysis, is a key floral integrator gene and eviction of H2A.Z-containing nucleosomes leads to *FT* upregulation (Kumar et al., 2012; Kumar and Wigge, 2010). Consequently, we found that *SWC4* downregulation results in increased *FT* expression due to a reduction in H2A.Z levels at *FT* nucleosome +1, and suggests that SWC4 negatively regulates *FT* expression by modulating H2A.Z deposition. Further, our

findings indicate that SWC4 is required for ARP6 targeting at *FT* chromatin (Supplemental Figure S21), supporting a key role for SWC4 in recruiting SWR1-C to this locus.

Our data represent the first evidence showing that a SWC4 homologue may bind DNA, reveal a novel regulator of the floral integrator *FT* and of other key transcription factors, and suggest a model in which *Arabidopsis* SWR1-C targets specific chromatin regions through SWC4 (Figure 8E). Yeast SWR1-C preferentially binds to long nucleosome-free AT-rich DNA regions and the adjoining nucleosome core particle, allowing discrimination of gene promoters over gene bodies (Ranjan et al., 2013; Yen et al., 2013). In this context, it would be very interesting to address if SWC4 DNA binding activity is conserved across eukaryotes and might contribute, together with additional proteins such as SWC2 (Yen et al., 2013), to the preferential recognition of specific chromatin locations in target genes.

METHODS

Genetic stocks and growth conditions

Arabidopsis thaliana swc4-1 (GABI_696G09) mutant seeds were obtained from the Nottingham *Arabidopsis* Stock Centre (NASC). Plants growing conditions and identification of *swc6-1* mutant were as described (Lazaro et al., 2008). LD conditions consisted of 16 h of light followed by 8 h of darkness; SD conditions consisted of 8 h of light followed by 16 h of darkness.

Generation of transgenic *SWC4* silenced and overexpressor lines.

SWC4 RNA interference construct consisted of the first 500 bp of *SWC4* coding region inserted twice into the vector pKANNIBAL (CSIRO, Australia) in opposite direction with an intron between them to create a hairpin. The full construct was then cloned into the binary vector pROK2 and transformed into WT plants to

generate the *swc4i* silenced plants. The overexpression construct in the pROK2 vector consisted of the full-length *SWC4* coding region under the control of the 35S promoter cloned into the pROK2 vector.. Transgenic plants were generated following *Agrobacterium tumefaciens*-mediated transformation using the floral-dip method (Clough and Bent, 1998).

Complementation of the *swc4-1* mutation

Homozygous *swc4-1* condition could not be obtained from self-fertilized *swc4-1/+* heterozygous plants that always segregated WT and *swc4-1/+* plants. To complement *swc4-1* lethality, first a second T-DNA insertion present in GABI_696G09 line was segregated away. Then a 5.9 kb genomic fragment including 1 kb upstream, 1.6 kb downstream and full *SWC4* gene was cloned into pCambia2300 binary vector (<http://www.cambia.org>). This genomic construct was transformed into *swc4-1/+* heterozygous plants by agro-infiltration. T1 transgenic lines were selected in media containing kanamycin (resistance in the pCambia 2300 vector) and sulfadiazine (resistance linked to the *swc4-1* T-DNA). Five out of six transgenic lines complemented the *swc4-1* allele: T2 and T3 progeny were 100% resistance to sulfadiazine, demonstrating that *swc4-1* lethality was fully rescued, allowing the maintenance of the *swc4-1* mutation in homozygosis in the presence of a transgenic *SWC4* WT genomic clone.

Phenotypic analyses

Flowering time was quantified by counting the total leaf number at the time of first flower opening. Root length was measured at 15 days after germination in vertical Petri dishes containing MS medium supplemented with 1% (w/v) sucrose and 1% (w/v) plant agar. Pollen grains (n>50) viability was observed under light microscope after Alexander's staining (Alexander, 1969). Nuclear visualization was done under UV epi-illumination after DAPI (4, 6-diamidino- 2-phenylindole) staining (0.1 µg/mL) for 1 h. Samples were washed and analyzed by fluorescence microscopy.

Microscopy

For white light microscopic analysis, rosette leaves were incubated in 95% ethanol at 90°C for 5 min and in lactophenol overnight at room temperature. Samples were mounted on slides and analyzed by Nomarski microscopy. For SEM, a Zeiss 960 microscope was used in low vacuum conditions with unfixed material. The cells were counted from three different leaf areas. The Digital images were analysed by software ImageJ 1.34s (Wayne Rasband, NIH, USA).

Flow cytometry

Rossete leaves were grinded and resuspended in cold nuclear isolation buffer as described (Galbraith et al., 1991). This crude preparation of isolated nuclei was filtered through 48-µm nylon mesh, treated with RNase A (100 µg/mL), and stained with propidium iodide (50 µg/mL; Sigma). At least 10⁴ isolated nuclei were analyzed with a FACScalibur flow cytometer (BD Bioscience).

Expression analyses

Total RNA was extracted from plant leaves or seedlings using EZNA Plant RNA Kit (Omega Bio-tek) following the manufacturer's recommendations. cDNA was prepared by reverse transcription of total RNA according to standard procedures (Martin-Trillo et al., 2006). *SWC4* transcript levels were assayed by quantitative radioactive RT-PCR experiments with specific primers designed to amplify *SWC4* N-terminal coding sequence (Supplemental Table S1). *UBIQUITIN 10 (UBQ 10)* was used as a loading control. Non-saturated RT-PCR products were blotted to Hybond-N+ (GE Healthcare) membranes following manufacturer instructions. *SWC4* and *UBQ10* DNA probes were PCR-amplified, purified and radioactively labelled with α-32P-dCTP using “Rediprime II DNA Random Prime Labelling system” (GE Healthcare). Nucleic acid hybridizations were performed following standard laboratory procedures and signal was detected using “Amersham Hyperfilm MP” (GE Healthcare). Gene expression analyses of flowering time regulator genes (*FLC*, *FT* and *SOC1*) and *SWC4* were performed by real time quantitative RT-PCR using LightCycler 480 SYBR Green (Roche). The specific primers used are described in the Supplemental Table S1.

RNA-seq analysis

Two biological replicates from each genotype, WT and *swc4i*, were sequenced and analyzed (Supplemental Table S2). Total RNA was extracted from 16 day-old seedling grown on agar plates under SD at Zeitgeber time (ZT) 8. Genomic DNA was removed with *Turbo DNase* (Ambion). Library preparation and sequencing were performed by Beijing Genomics Institute (HiSeq2000, 100 bp pair-end sequencing, 200 bp short-insert library). Reads were mapped using TOPHAT 2.1.0 (Trapnell et al., 2009) in Galaxy (Afgan et al., 2016) and differential expression analysis was performed using DESeq2 module (Love et al., 2014) of SeqMonk software (<http://www.bioinformatics.babraham.ac.uk/projects/seqmonk/>). Gene Ontology analysis was performed using AgriGO (Du et al., 2010) and REVIGO (Supek et al., 2011) web-based tools. Venn Diagrams were elaborated using VENNY (<http://bioinfogp.cnb.csic.es/tools/venny/index.html>).

Chromatin Immunoprecipitation

ChIP experiments were performed as described (Song et al., 2014), using 1.5 g of 16 day-old seedling grown on agar plates under SD collected at ZT8. ChIP DNA was quantified by Q-PCR using the oligonucleotides described in Supplemental Table S1. DNA enrichment was estimated as the fraction of immunoprecipitated DNA relative to input (%INPUT). Relative histone modifications levels were determined as %INPUT of each region / %INPUT *ACTIN* fragment. *Arabidopsis* specific α -HTA9 antibody (AS10718) from Agrisera was thoroughly tested by western blot and control ChIP experiments (Supplemental Figure S10 and Figure 7B). α -SWC4 antibody was raised against full length SWC4 protein obtained as described in Supplemental Methods. Data from Figure 7D and Fig 8A are from independent experiments. We also used the following antibodies: α -H4K5ac (07-327 Merck-Millipore), α -H3 (Abcam ab1791), α -HTA9/11 (Zhang et al., 2015) and α -ARP6 (Zhao et al., 2018).

ChIP-seq analysis

Two independent ChIP experiments using α -HTA9 and α -H3 antibodies (16 day-old seedlings, grown under SD, collected at ZT8) of each genotype, WT and *swc4i*, were sequenced and analyzed (Supplemental Table S3). ChIP-seq libraries were generated using the Ovation Ultralow Library System V2 (NuGEN), library size 300-400 bp using 10 ng of starting material. Sequencing was performed on a HiSeq2500, with single-end reads 50 bp length. Reads from independent biological replicates were mapped to the TAIR10 genome using Bowtie (v 2) replicate wise (Langmead et al., 2009). Delineation of significantly ChIP-enriched regions and differential analysis between WT and *swc4i* were done with SICER (Zang et al., 2009) using H3 as control library with a redundancy threshold of 1, a window size of 200bp, a gap size of 600bp and FDR=0.01. Heatmap of the HTA9 ChIP-seq signal over the TSS was created using deepTools suite (Ramirez et al., 2014). For metagene plots, ChIP signals were normalized with H3 ChIP data by calculating the difference in 150-bp bins across the genome. These data were standardized and normalized for comparative purposes across samples with a z-score transformation (Cheadle et al., 2003). Annotations of peak location relative to different genomic features were performed using PAVIS (Huang et al., 2013).

Protein-binding microarrays

SWC4 DNA-binding specificity was determined by performing protein-binding microarrays. Detection of protein-DNA complexes, data processing and analysis of enriched 8-mers were performed as described (Franco-Zorrilla et al., 2014; Godoy et al., 2011). See Supplemental METHODS for detailed method description.

Bioinformatics analyses of SWC4 AT-rich DNA binding elements

Position weight matrices for the AT-rich DNA elements were used to scan the regions surrounding the TSS (from -500 to +500) with Regulatory Sequence Analysis Tools (RSAT) (Medina-Rivera et al., 2015). Data corresponding to *scw4i* up-regulated with low H2A.Z and all TAIR10 genes were extracted and binding sites densities scored as the number of binding sites/number of promoters.

Yeast two-hybrid analysis

Y2H interaction analyses were conducted in the yeast strain Y190 with the MatchMaker two-hybrid system (Clontech). pGBT8 or pDEST32 plasmids were used for GBD fusion constructs and pGAD or pDEST22 plasmids were used for GAD fusion constructs. cDNAs for *SWC4*, *SWC6* and *YAF9A* were obtained by standard PCR techniques and cloned into the above-mentioned vectors using Gateway gene cloning technologies (Invitrogen). Selection of yeasts was performed on synthetic complete minimal medium without His, Leu, and Trp, supplemented with 0 to 25 mM 3-amino-1,2,4-triazole (3-AT).

Co-IP studies

Co-IP experiments in *N. benthamiana* were performed as described in (Lazaro et al., 2015). Briefly, *SWC4* full-length cDNA was cloned using Gateway recombinant technologies (Life Technologies) into the pGWB5 or pGWB6 vectors; *SWC6*-myc construct is described in (Lazaro et al., 2008); and. *SWC4*-GFP fusion proteins were immunoprecipitated with GFP-Trap_A (ChromoTek) and *SWC6*-myc was detected using anti c-Myc (Millipore, clone 4A6).

Protein affinity purification and tandem mass spectrometry

Functional and complemented *Arabidopsis* *SWC6*-Myc overexpressing lines were used in these assays (Lazaro et al., 2008). Proteins were extracted from 5 g of 10 day-old *Arabidopsis* seedlings, and *SWC6*-Myc was immunoprecipitated using a c-Myc antibody-conjugated agarose beads (MBL CODE No. 3305A, MoAb. Clone 1G4). This mild purification system allowed c-Myc peptide elution of specific interactors reducing the number of interacting proteins due to non-specific binding to the agarose beads. Extraction and immunoprecipitation were performed at 4°C using the same buffer (Tris-HCl pH7.5 10 mM, NaCl 150 mM, EDTA 2.5 mM, Glycerol 10% and Triton X-100 0.5%, supplemented with ROCHE Complete protease inhibitors)

c-Myc-eluted and agarose beads protein samples were analyzed by tandem mass spectrometry (AP-MS/MS). Detailed procedures descriptions are in Supplemental

METHODS. Specific SWC6 interactors were identified comparing the results obtained using SWC6-Myc tagged lines and control *Arabidopsis* plants without the tag. We performed two independent experiments and proteins identified in both independent SWC6-Myc purifications are listed in Supplemental Data S1.

See Supplemental METHODS for detailed description of protein-interaction analysis and further methods.

ACCESSION NUMBERS

The datasets generated during the current study are available in the NCBI Sequence Read Archive (SRA) repository under accession numbers SRP133545 (ChIP-seq) and SRP133496 (RNA-seq).

SUPPLEMENTAL INFORMATION

Supplemental Information is available at Molecular Plant Online

FUNDING

This work was supported by grants BIO2010-15589, BIO2013-43098-R, and BIO2016-77559-R to JAJ and MP and grant RYC-2013-14689 to PC from the Spanish Ministerio de Economía y Competitividad (MINECO/FEDER, EU), and *Marie Curie* FP7-PEOPLE-2011-IEF grant 298790 to PC and JAJ from the European Commission. The CBGP is a Severo Ochoa Center of Excellence (SEV-2016-0672). The CNIC is supported by the Ministry of Economy, Industry and Competitiveness (MEIC) and the Pro CNIC Foundation, and is also a Severo Ochoa Center of Excellence (SEV-2015-0505).

AUTHORS CONTRIBUTIONS

MP and JAJ designed the research; AGZ performed *swc4-1* mutant isolation, generated and characterized *swc4i* knockdown and *SWC4* overexpression lines, and carried out the Y2H and BiFC analyses; PC performed *swc4-1* complementation, SWC6 protein purification, *swc4i* RNA-seq, ChIP and ChIP-seq experiments; JMR and JSG performed library preparation and ChIP-seq analysis; SJ tested α -SWC4 antibody; PR and CK characterized *swc4-1* embryo lethality; JAL and JV performed the proteomics analysis; and JMFZ and RS carried out the protein-binding microarray assay. PC, MP and JAJ analysed all the data and wrote the paper. All authors read and approve the final manuscript.

ACKNOWLEDGMENTS

We thank Federico Valverde and Alicia Orea (IBVF, Seville) for help with BiFC studies and confocal microscopy; Crisanto Gutiérrez (CIB, Madrid), Elena Ramírez (CBGP, Madrid) for their advice with flow cytometry experiments. Alejandro Ferrando (IBMCP, Valencia) for the BiFC vectors. List of genes misregulated in *h2a.z* mutant was provided by Daniel Zilberman (UCLA, Los Angeles); α -HTA9/11 was a kind gift from Aiwu Dong (Fudan University, Shanghai) and α -ARP6 was kindly provided by Roger Deal, Emory University, Atlanta, GA). We thank Jenifer Pozas (CBGP, Madrid) y Raquel Mesa (CNIC, Madrid) for her technical assistance, and Dr. Mark Wilkinson for his help editing the manuscript. The authors declare that they have no conflict of interest.

REFERENCES

- Aasland, R., Stewart, A.F., and Gibson, T.** (1996). The SANT domain: a putative DNA-binding domain in the SWI-SNF and ADA complexes, the transcriptional co-repressor N-CoR and TFIIB. *Trends Biochem Sci* **21**, 87-88.
- Afgan, E., Baker, D., van den Beek, M., Blankenberg, D., Bouvier, D., Cech, M., Chilton, J., Clements, D., Coraor, N., Eberhard, C., et al.** (2016). The Galaxy platform for accessible, reproducible and collaborative biomedical analyses: 2016 update. *Nucleic Acids Res* **44**, W3-W10.
- Alexander, M.P.** (1969). Differential staining of aborted and nonaborted pollen. *Stain Technol* **44**, 117-122.
- Andres, F., and Coupland, G.** (2012). The genetic basis of flowering responses to seasonal cues. *Nat Rev Genet* **13**, 627-639.
- Auger, A., Galarneau, L., Altaf, M., Nourani, A., Doyon, Y., Utley, R.T., Cronier, D., Allard, S., and Cote, J.** (2008). Eaf1 is the platform for NuA4 molecular assembly that evolutionarily links chromatin acetylation to ATP-dependent exchange of histone H2A variants. *Mol Cell Biol* **28**, 2257-2270.
- Berger, M.F., and Bulyk, M.L.** (2009). Universal protein-binding microarrays for the comprehensive characterization of the DNA-binding specificities of transcription factors. *Nat Protoc* **4**, 393-411.
- Berriri, S., Gangappa, S.N., and Kumar, S.V.** (2016). SWR1 Chromatin-Remodeling Complex Subunits and H2A.Z Have Non-overlapping Functions in Immunity and Gene Regulation in Arabidopsis. *Mol Plant* **9**, 1051-1065.
- Bieluszewski, T., Galganski, L., Sura, W., Bieluszewska, A., Abram, M., Ludwikow, A., Ziolkowski, P.A., and Sadowski, J.** (2015). AtEAF1 is a potential platform protein for Arabidopsis NuA4 acetyltransferase complex. *BMC Plant Biol* **15**, 75.
- Billon, P., and Cote, J.** (2012). Precise deposition of histone H2A.Z in chromatin for genome expression and maintenance. *Biochim Biophys Acta* **1819**, 290-302.
- Bittner, C.B., Zeisig, D.T., Zeisig, B.B., and Slany, R.K.** (2004). Direct physical and functional interaction of the NuA4 complex components Yaf9p and Swc4p. *Eukaryot Cell* **3**, 976-983.
- Boyer, L.A., Langer, M.R., Crowley, K.A., Tan, S., Denu, J.M., and Peterson, C.L.** (2002). Essential role for the SANT domain in the functioning of multiple chromatin remodeling enzymes. *Mol Cell* **10**, 935-942.
- Boyer, L.A., Latek, R.R., and Peterson, C.L.** (2004). The SANT domain: a unique histone-tail-binding module? *Nat Rev Mol Cell Biol* **5**, 158-163.
- Cai, H., Zhao, L., Wang, L., Zhang, M., Su, Z., Cheng, Y., Zhao, H., and Qin, Y.** (2017). ERECTA signaling controls Arabidopsis inflorescence architecture through chromatin-mediated activation of PRE1 expression. *New Phytol* **214**, 1579-1596.
- Clough, S.J., and Bent, A.F.** (1998). Floral dip: a simplified method for Agrobacterium-mediated transformation of Arabidopsis thaliana. *Plant J* **16**, 735-743.
- Coleman-Derr, D., and Zilberman, D.** (2012a). Deposition of histone variant H2A.Z within gene bodies regulates responsive genes. *PLoS Genet* **8**, e1002988.
- Coleman-Derr, D., and Zilberman, D.** (2012b). DNA methylation, H2A.Z, and the regulation of constitutive expression. *Cold Spring Harb Symp Quant Biol* **77**, 147-154.
- Costas, C., de la Paz Sanchez, M., Stroud, H., Yu, Y., Oliveros, J.C., Feng, S., Benguria, A., Lopez-Vidriero, I., Zhang, X., Solano, R., et al.** (2011). Genome-wide mapping of Arabidopsis thaliana origins of DNA replication and their associated epigenetic marks. *Nat Struct Mol Biol* **18**, 395-400.

- Cheadle, C., Vawter, M.P., Freed, W.J., and Becker, K.G.** (2003). Analysis of microarray data using Z score transformation. *J Mol Diagn* **5**, 73-81.
- Choi, K., Kim, J., Muller, S.Y., Oh, M., Underwood, C., Henderson, I., and Lee, I.** (2016). Regulation of MicroRNA-Mediated Developmental Changes by the SWR1 Chromatin Remodeling Complex. *Plant Physiol* **171**, 1128-1143.
- Choi, K., Kim, S., Kim, S.Y., Kim, M., Hyun, Y., Lee, H., Choe, S., Kim, S.G., Michaels, S., and Lee, I.** (2005). SUPPRESSOR OF FRIGIDA3 encodes a nuclear ACTIN-RELATED PROTEIN6 required for floral repression in Arabidopsis. *Plant Cell* **17**, 2647-2660.
- Choi, K., Park, C., Lee, J., Oh, M., Noh, B., and Lee, I.** (2007). Arabidopsis homologs of components of the SWR1 complex regulate flowering and plant development. *Development* **134**, 1931-1941.
- Choi, K., Zhao, X., Kelly, K.A., Venn, O., Higgins, J.D., Yelina, N.E., Hardcastle, T.J., Ziolkowski, P.A., Copenhaver, G.P., Franklin, F.C., et al.** (2013). Arabidopsis meiotic crossover hot spots overlap with H2A.Z nucleosomes at gene promoters. *Nat Genet* **45**, 1327-1336.
- Dai, X., Bai, Y., Zhao, L., Dou, X., Liu, Y., Wang, L., Li, Y., Li, W., Hui, Y., Huang, X., et al.** (2017). H2A.Z Represses Gene Expression by Modulating Promoter Nucleosome Structure and Enhancer Histone Modifications in Arabidopsis. *Mol Plant* **10**, 1274-1292.
- Deal, R.B., and Henikoff, S.** (2011). Histone variants and modifications in plant gene regulation. *Curr Opin Plant Biol* **14**, 116-122.
- Deal, R.B., Kandasamy, M.K., McKinney, E.C., and Meagher, R.B.** (2005). The nuclear actin-related protein ARP6 is a pleiotropic developmental regulator required for the maintenance of FLOWERING LOCUS C expression and repression of flowering in Arabidopsis. *Plant Cell* **17**, 2633-2646.
- Deal, R.B., Topp, C.N., McKinney, E.C., and Meagher, R.B.** (2007). Repression of flowering in Arabidopsis requires activation of FLOWERING LOCUS C expression by the histone variant H2A.Z. *Plant Cell* **19**, 74-83.
- Dhillon, N., Oki, M., Szyjka, S.J., Aparicio, O.M., and Kamakaka, R.T.** (2006). H2A.Z functions to regulate progression through the cell cycle. *Mol Cell Biol* **26**, 489-501.
- Doyon, Y., and Cote, J.** (2004). The highly conserved and multifunctional NuA4 HAT complex. *Curr Opin Genet Dev* **14**, 147-154.
- Doyon, Y., Selleck, W., Lane, W.S., Tan, S., and Cote, J.** (2004). Structural and functional conservation of the NuA4 histone acetyltransferase complex from yeast to humans. *Mol Cell Biol* **24**, 1884-1896.
- Du, Z., Zhou, X., Ling, Y., Zhang, Z., and Su, Z.** (2010). agriGO: a GO analysis toolkit for the agricultural community. *Nucleic Acids Res* **38**, W64-70.
- Earley, K.W., Shook, M.S., Brower-Toland, B., Hicks, L., and Pikaard, C.S.** (2007). In vitro specificities of Arabidopsis co-activator histone acetyltransferases: implications for histone hyperacetylation in gene activation. *Plant J* **52**, 615-626.
- Faast, R., Thonglairoam, V., Schulz, T.C., Beall, J., Wells, J.R., Taylor, H., Matthaei, K., Rathjen, P.D., Tremethick, D.J., and Lyons, I.** (2001). Histone variant H2A.Z is required for early mammalian development. *Curr Biol* **11**, 1183-1187.
- Ferrandiz, C., and Fourquin, C.** (2014). Role of the FUL-SHP network in the evolution of fruit morphology and function. *Journal of experimental botany* **65**, 4505-4513.
- Franco-Zorrilla, J.M., Lopez-Vidriero, I., Carrasco, J.L., Godoy, M., Vera, P., and Solano, R.** (2014). DNA-binding specificities of plant transcription factors and their potential to define target genes. *Proc Natl Acad Sci U S A* **111**, 2367-2372.
- Galbraith, D.W., Harkins, K.R., and Knapp, S.** (1991). Systemic Endopolyploidy in Arabidopsis thaliana. *Plant Physiol* **96**, 985-989.

Gentry, M., and Hennig, L. (2014). Remodelling chromatin to shape development of plants. *Exp Cell Res* **321**, 40-46.

Gerhold, C.B., and Gasser, S.M. (2014). INO80 and SWR complexes: relating structure to function in chromatin remodeling. *Trends Cell Biol* **24**, 619-631.

Godoy, M., Franco-Zorrilla, J.M., Perez-Perez, J., Oliveros, J.C., Lorenzo, O., and Solano, R. (2011). Improved protein-binding microarrays for the identification of DNA-binding specificities of transcription factors. *Plant J* **66**, 700-711.

Gonzalez, N., Vanhaeren, H., and Inze, D. (2012). Leaf size control: complex coordination of cell division and expansion. *Trends Plant Sci* **17**, 332-340.

Gu, Q., Ferrandiz, C., Yanofsky, M.F., and Martienssen, R. (1998). The FRUITFULL MADS-box gene mediates cell differentiation during Arabidopsis fruit development. *Development* **125**, 1509-1517.

Guillemette, B., Bataille, A.R., Gevry, N., Adam, M., Blanchette, M., Robert, F., and Gaudreau, L. (2005). Variant histone H2A.Z is globally localized to the promoters of inactive yeast genes and regulates nucleosome positioning. *PLoS Biol* **3**, e384.

Ho, L., and Crabtree, G.R. (2010). Chromatin remodelling during development. *Nature* **463**, 474-484.

Holt, B.F., 3rd, Boyes, D.C., Ellerstrom, M., Siefers, N., Wiig, A., Kauffman, S., Grant, M.R., and Dangl, J.L. (2002). An evolutionarily conserved mediator of plant disease resistance gene function is required for normal Arabidopsis development. *Dev Cell* **2**, 807-817.

Huang, W., Loganantharaj, R., Schroeder, B., Fargo, D., and Li, L. (2013). PAVIS: a tool for Peak Annotation and Visualization. *Bioinformatics* **29**, 3097-3099.

Hwan Lee, J., Joon Kim, J., and Ahn, J.H. (2012). Role of SEPALLATA3 (SEP3) as a downstream gene of miR156-SPL3-FT circuitry in ambient temperature-responsive flowering. *Plant Signal Behav* **7**, 1151-1154.

Jarillo, J.A., and Pineiro, M. (2015). H2A.Z mediates different aspects of chromatin function and modulates flowering responses in Arabidopsis. *Plant J* **83**, 96-109.

Jiang, D., and Berger, F. (2017). Histone variants in plant transcriptional regulation. *Biochim Biophys Acta* **1860**, 123-130.

Kalocsay, M., Hiller, N.J., and Jentsch, S. (2009). Chromosome-wide Rad51 spreading and SUMO-H2A.Z-dependent chromosome fixation in response to a persistent DNA double-strand break. *Mol Cell* **33**, 335-343.

Kandasamy, M.K., Deal, R.B., McKinney, E.C., and Meagher, R.B. (2005). Silencing the nuclear actin-related protein AtARP4 in Arabidopsis has multiple effects on plant development, including early flowering and delayed floral senescence. *Plant J* **41**, 845-858.

Kandasamy, M.K., McKinney, E.C., and Meagher, R.B. (2008). ACTIN-RELATED PROTEIN8 encodes an F-box protein localized to the nucleolus in Arabidopsis. *Plant Cell Physiol* **49**, 858-863.

Kapoor, P., and Shen, X. (2014). Mechanisms of nuclear actin in chromatin-remodeling complexes. *Trends Cell Biol* **24**, 238-246.

Kardailsky, I., Shukla, V.K., Ahn, J.H., Dagenais, N., Christensen, S.K., Nguyen, J.T., Chory, J., Harrison, M.J., and Weigel, D. (1999). Activation tagging of the floral inducer *FT*. *Science* **286**, 1962-1965.

Kawashima, T., Lorkovic, Z.J., Nishihama, R., Ishizaki, K., Axelsson, E., Yelagandula, R., Kohchi, T., and Berger, F. (2015). Diversification of histone H2A variants during plant evolution. *Trends Plant Sci* **20**, 419-425.

Kobor, M.S., Venkatasubrahmanyam, S., Meneghini, M.D., Gin, J.W., Jennings, J.L., Link, A.J., Madhani, H.D., and Rine, J. (2004). A protein complex containing the conserved Swi2/Snf2-related ATPase Swr1p deposits histone variant H2A.Z into euchromatin. *PLoS Biol* **2**, E131.

Krogan, N.J., Baetz, K., Keogh, M.C., Datta, N., Sawa, C., Kwok, T.C., Thompson, N.J., Davey, M.G., Pootoolal, J., Hughes, T.R., et al. (2004). Regulation of chromosome stability by the histone H2A variant Htz1, the Swr1 chromatin remodeling complex, and the histone acetyltransferase NuA4. *Proc Natl Acad Sci U S A* **101**, 13513-13518.

Kumar, S.V., Lucyshyn, D., Jaeger, K.E., Alos, E., Alvey, E., Harberd, N.P., and Wigge, P.A. (2012). Transcription factor PIF4 controls the thermosensory activation of flowering. *Nature* **484**, 242-245.

Kumar, S.V., and Wigge, P.A. (2010). H2A.Z-containing nucleosomes mediate the thermosensory response in Arabidopsis. *Cell* **140**, 136-147.

Langmead, B., Trapnell, C., Pop, M., and Salzberg, S.L. (2009). Ultrafast and memory-efficient alignment of short DNA sequences to the human genome. *Genome Biol* **10**, R25.

Latrasse, D., Benhamed, M., Henry, Y., Domenichini, S., Kim, W., Zhou, D.X., and Delarue, M. (2008). The MYST histone acetyltransferases are essential for gametophyte development in Arabidopsis. *BMC Plant Biol* **8**, 121.

Lazaro, A., Gomez-Zambrano, A., Lopez-Gonzalez, L., Pineiro, M., and Jarillo, J.A. (2008). Mutations in the Arabidopsis SWC6 gene, encoding a component of the SWR1 chromatin remodelling complex, accelerate flowering time and alter leaf and flower development. *J Exp Bot* **59**, 653-666.

Lazaro, A., Mouriz, A., Pineiro, M., and Jarillo, J.A. (2015). Red Light-Mediated Degradation of CONSTANS by the E3 Ubiquitin Ligase HOS1 Regulates Photoperiodic Flowering in Arabidopsis. *Plant Cell* **27**, 2437-2454.

Li, X., Yu, E., Fan, C., Zhang, C., Fu, T., and Zhou, Y. (2012). Developmental, cytological and transcriptional analysis of autotetraploid Arabidopsis. *Planta* **236**, 579-596.

Liu, X., and Gorovsky, M.A. (1996). Cloning and characterization of the major histone H2A genes completes the cloning and sequencing of known histone genes of Tetrahymena thermophila. *Nucleic Acids Res* **24**, 3023-3030.

Love, M.I., Huber, W., and Anders, S. (2014). Moderated estimation of fold change and dispersion for RNA-seq data with DESeq2. *Genome Biol* **15**, 550.

Lu, P.Y., Levesque, N., and Kobor, M.S. (2009). NuA4 and SWR1-C: two chromatin-modifying complexes with overlapping functions and components. *Biochem Cell Biol* **87**, 799-815.

March-Diaz, R., Garcia-Dominguez, M., Florencio, F.J., and Reyes, J.C. (2007). SEF, a new protein required for flowering repression in Arabidopsis, interacts with PIE1 and ARP6. *Plant Physiol* **143**, 893-901.

March-Diaz, R., Garcia-Dominguez, M., Lozano-Juste, J., Leon, J., Florencio, F.J., and Reyes, J.C. (2008). Histone H2A.Z and homologues of components of the SWR1 complex are required to control immunity in Arabidopsis. *The Plant Journal* **53**, 475-487.

March-Diaz, R., and Reyes, J.C. (2009). The beauty of being a variant: H2A.Z and the SWR1 complex in plants. *Molecular Plant* **2**, 565-577.

Marques, M., Laflamme, L., Gervais, A.L., and Gaudreau, L. (2010). Reconciling the positive and negative roles of histone H2A.Z in gene transcription. *Epigenetics* **5**, 267-272.

Martin-Trillo, M., Lazaro, A., Poethig, R.S., Gomez-Mena, C., Pineiro, M.A., Martinez-Zapater, J.M., and Jarillo, J.A. (2006). EARLY IN SHORT DAYS 1 (ESD1) encodes ACTIN-RELATED PROTEIN 6 (AtARP6), a putative component of chromatin remodelling complexes that positively regulates FLC accumulation in Arabidopsis. *Development* **133**, 1241-1252.

Maruyama, Y., Yamoto, N., Suzuki, Y., Chiba, Y., Yamazaki, K., Sato, T., and Yamaguchi, J. (2013). The Arabidopsis transcriptional repressor ERF9 participates in resistance against necrotrophic fungi. *Plant Sci* **213**, 79-87.

Mavrich, T.N., Jiang, C., Ioshikhes, I.P., Li, X., Venters, B.J., Zanton, S.J., Tomsho, L.P., Qi, J., Glaser, R.L., Schuster, S.C., et al. (2008). Nucleosome organization in the Drosophila genome. *Nature* **453**, 358-362.

Meagher, R.B., Kandasamy, M.K., Deal, R.B., and McKinney, E.C. (2007). Actin-related proteins in chromatin-level control of the cell cycle and developmental transitions. *Trends Cell Biol* **17**, 325-332.

Medina-Rivera, A., Defrance, M., Sand, O., Herrmann, C., Castro-Mondragon, J.A., Delerce, J., Jaeger, S., Blanchet, C., Vincens, P., Caron, C., et al. (2015). RSAT 2015: Regulatory Sequence Analysis Tools. *Nucleic Acids Res* **43**, W50-56.

Micialkiewicz, A., and Chelstowska, A. (2008). The essential function of Swc4p - a protein shared by two chromatin-modifying complexes of the yeast *Saccharomyces cerevisiae* - resides within its N-terminal part. *Acta Biochim Pol* **55**, 603-612.

Millar, C.B., Xu, F., Zhang, K., and Grunstein, M. (2006). Acetylation of H2AZ Lys 14 is associated with genome-wide gene activity in yeast. *Genes Dev* **20**, 711-722.

Mizuguchi, G., Shen, X., Landry, J., Wu, W.H., Sen, S., and Wu, C. (2004). ATP-driven exchange of histone H2AZ variant catalyzed by SWR1 chromatin remodeling complex. *Science* **303**, 343-348.

Mohan, K.N., Ding, F., and Chaillet, J.R. (2011). Distinct roles of DMAP1 in mouse development. *Mol Cell Biol* **31**, 1861-1869.

Moon, J., Suh, S.S., Lee, H., Choi, K.R., Hong, C.B., Paek, N.C., Kim, S.G., and Lee, I. (2003). The SOC1 MADS-box gene integrates vernalization and gibberellin signals for flowering in Arabidopsis. *Plant J* **35**, 613-623.

Nguyen, V.Q., Ranjan, A., Stengel, F., Wei, D., Aebersold, R., Wu, C., and Leschziner, A.E. (2013). Molecular architecture of the ATP-dependent chromatin-remodeling complex SWR1. *Cell* **154**, 1220-1231.

Noh, Y.S., and Amasino, R.M. (2003). PIE1, an ISWI family gene, is required for FLC activation and floral repression in Arabidopsis. *Plant Cell* **15**, 1671-1682.

Qin, Y., Zhao, L., Skaggs, M.I., Andreuzza, S., Tsukamoto, T., Panoli, A., Wallace, K.N., Smith, S., Siddiqi, I., Yang, Z., et al. (2014). ACTIN-RELATED PROTEIN6 Regulates Female Meiosis by Modulating Meiotic Gene Expression in Arabidopsis. *Plant Cell* **26**, 1612-1628.

Raisner, R.M., Hartley, P.D., Meneghini, M.D., Bao, M.Z., Liu, C.L., Schreiber, S.L., Rando, O.J., and Madhani, H.D. (2005). Histone variant H2A.Z marks the 5' ends of both active and inactive genes in euchromatin. *Cell* **123**, 233-248.

Ramirez, F., Dundar, F., Diehl, S., Gruning, B.A., and Manke, T. (2014). deepTools: a flexible platform for exploring deep-sequencing data. *Nucleic Acids Res* **42**, W187-191.

Rangasamy, D., Greaves, I., and Tremethick, D.J. (2004). RNA interference demonstrates a novel role for H2A.Z in chromosome segregation. *Nat Struct Mol Biol* **11**, 650-655.

Ranjan, A., Mizuguchi, G., FitzGerald, P.C., Wei, D., Wang, F., Huang, Y., Luk, E., Woodcock, C.L., and Wu, C. (2013). Nucleosome-free region dominates histone acetylation in targeting SWR1 to promoters for H2A.Z replacement. *Cell* **154**, 1232-1245.

Rosa, M., Von Harder, M., Cigliano, R.A., Schlogelhofer, P., and Mittelsten Scheid, O. (2013). The Arabidopsis SWR1 chromatin-remodeling complex is important for DNA repair, somatic recombination, and meiosis. *Plant Cell* **25**, 1990-2001.

Rountree, M.R., Bachman, K.E., and Baylin, S.B. (2000). DNMT1 binds HDAC2 and a new co-repressor, DMAP1, to form a complex at replication foci. *Nat Genet* **25**, 269-277.

Ryan, D.P., Sundaramoorthy, R., Martin, D., Singh, V., and Owen-Hughes, T. (2011). The DNA-binding domain of the Chd1 chromatin-remodelling enzyme contains SANT and SLIDE domains. *EMBO J* **30**, 2596-2609.

Sadeghi, L., Bonilla, C., Stralfors, A., Ekwall, K., and Svensson, J.P. (2011). Podbat: a novel genomic tool reveals Swr1-independent H2A.Z incorporation at gene coding sequences through epigenetic meta-analysis. *PLoS Comput Biol* **7**, e1002163.

Shani, E., Salehin, M., Zhang, Y., Sanchez, S.E., Doherty, C., Wang, R., Mangado, C.C., Song, L., Tal, I., Pisanty, O., et al. (2017). Plant Stress Tolerance Requires Auxin-Sensitive Aux/IAA Transcriptional Repressors. *Curr Biol* **27**, 437-444.

Smith, A.P., Jain, A., Deal, R.B., Nagarajan, V.K., Poling, M.D., Raghothama, K.G., and Meagher, R.B. (2010). Histone H2A.Z regulates the expression of several classes of phosphate starvation response genes but not as a transcriptional activator. *Plant Physiol* **152**, 217-225.

Song, J., Rutjens, B., and Dean, C. (2014). Detecting histone modifications in plants. *Methods Mol Biol* **1112**, 165-175.

Subramanian, V., Fields, P.A., and Boyer, L.A. (2015). H2A.Z: a molecular rheostat for transcriptional control. *F1000Prime Rep* **7**, 01.

Supek, F., Bosnjak, M., Skunca, N., and Smuc, T. (2011). REVIGO summarizes and visualizes long lists of gene ontology terms. *PLoS One* **6**, e21800.

Sura, W., Kabza, M., Karlowski, W.M., Bieluszewski, T., Kus-Slowinska, M., Paweloszek, L., Sadowski, J., and Ziolkowski, P.A. (2017). Dual Role of the Histone Variant H2A.Z in Transcriptional Regulation of Stress-Response Genes. *Plant Cell* **29**, 791-807.

Tahirov, T.H., Sasaki, M., Inoue-Bungo, T., Fujikawa, A., Sato, K., Kumasaka, T., Yamamoto, M., and Ogata, K. (2001). Crystals of ternary protein-DNA complexes composed of DNA-binding domains of c-Myb or v-Myb, C/EBPalpha or C/EBPbeta and tom-1A promoter fragment. *Acta Crystallogr D Biol Crystallogr* **57**, 1655-1658.

Talbert, P.B., and Henikoff, S. (2017). Histone variants on the move: substrates for chromatin dynamics. *Nat Rev Mol Cell Biol* **18**, 115-126.

Thatcher, T.H., and Gorovsky, M.A. (1994). Phylogenetic analysis of the core histones H2A, H2B, H3, and H4. *Nucleic Acids Res* **22**, 174-179.

Trapnell, C., Pachter, L., and Salzberg, S.L. (2009). TopHat: discovering splice junctions with RNA-Seq. *Bioinformatics* **25**, 1105-1111.

van Daal, A., and Elgin, S.C. (1992). A histone variant, H2AvD, is essential in *Drosophila melanogaster*. *Mol Biol Cell* **3**, 593-602.

Van Leene, J., Eeckhout, D., Cannoot, B., De Winne, N., Persiau, G., Van De Slijke, E., Vercruyse, L., Dedecker, M., Verkest, A., Vandepoele, K., et al. (2015). An improved toolbox to unravel the plant cellular machinery by tandem affinity purification of Arabidopsis protein complexes. *Nat Protocols* **10**, 169-187.

Venkatesh, S., and Workman, J.L. (2015). Histone exchange, chromatin structure and the regulation of transcription. *Nat Rev Mol Cell Biol* **16**, 178-189.

Wan, Y., Saleem, R.A., Ratushny, A.V., Roda, O., Smith, J.J., Lin, C.H., Chiang, J.H., and Aitchison, J.D. (2009). Role of the histone variant H2A.Z/Htz1p in TBP recruitment, chromatin dynamics, and regulated expression of oleate-responsive genes. *Mol Cell Biol* **29**, 2346-2358.

Weber, C.M., and Henikoff, S. (2014). Histone variants: dynamic punctuation in transcription. *Genes Dev* **28**, 672-682.

Weber, C.M., Ramachandran, S., and Henikoff, S. (2014). Nucleosomes are context-specific, H2A.Z-modulated barriers to RNA polymerase. *Mol Cell* **53**, 819-830.

Xiao, J., Zhang, H., Xing, L., Xu, S., Liu, H., Chong, K., and Xu, Y. (2013). Requirement of histone acetyltransferases HAM1 and HAM2 for epigenetic modification of FLC in regulating flowering in Arabidopsis. *J Plant Physiol* **170**, 444-451.

Yelagandula, R., Stroud, H., Holec, S., Zhou, K., Feng, S., Zhong, X., Muthurajan, U.M., Nie, X., Kawashima, T., Groth, M., et al. (2014). The histone variant H2A.W defines heterochromatin and promotes chromatin condensation in Arabidopsis. *Cell* **158**, 98-109.

Yen, K., Vinayachandran, V., and Pugh, B.F. (2013). SWR-C and INO80 chromatin remodelers recognize nucleosome-free regions near +1 nucleosomes. *Cell* **154**, 1246-1256.

Yi, H., Sardesai, N., Fujinuma, T., Chan, C.W., Veena, and Gelvin, S.B. (2006). Constitutive expression exposes functional redundancy between the Arabidopsis histone H2A gene HTA1 and other H2A gene family members. *Plant Cell* **18**, 1575-1589.

Zacharakis, V., Benhamed, M., Poulis, S., Latrassé, D., Papoutsoglou, P., Delarue, M., and Vlachonasios, K.E. (2012). The Arabidopsis ortholog of the YEATS domain containing protein YAF9a regulates flowering by controlling H4 acetylation levels at the *FLC* locus. *Plant Sci* **196**, 44-52.

Zang, C., Schones, D.E., Zeng, C., Cui, K., Zhao, K., and Peng, W. (2009). A clustering approach for identification of enriched domains from histone modification ChIP-Seq data. *Bioinformatics* **25**, 1952-1958.

Zhang, C., Cao, L., Rong, L., An, Z., Zhou, W., Ma, J., Shen, W.-H., Zhu, Y., and Dong, A. (2015). The chromatin-remodeling factor AtINO80 plays crucial roles in genome stability maintenance and in plant development. *The Plant Journal* **82**, 655-668.

Zhang, H., Roberts, D.N., and Cairns, B.R. (2005). Genome-wide dynamics of Htz1, a histone H2A variant that poises repressed/basal promoters for activation through histone loss. *Cell* **123**, 219-231.

Zhao, L., Cai, H., Su, Z., Wang, L., Huang, X., Zhang, M., Chen, P., Dai, X., Zhao, H., Palanivelu, R., et al. (2018). KLU suppresses megasporocyte cell fate through SWR1-mediated activation of WRKY28 expression in Arabidopsis. *Proc Natl Acad Sci U S A* **115**, E526-E535.

Zhou, B.O., Wang, S.S., Xu, L.X., Meng, F.L., Xuan, Y.J., Duan, Y.M., Wang, J.Y., Hu, H., Dong, X., Ding, J., et al. (2010). SWR1 complex poises heterochromatin boundaries for antisilencing activity propagation. *Mol Cell Biol* **30**, 2391-2400.

Zilberman, D., Coleman-Derr, D., Ballinger, T., and Henikoff, S. (2008). Histone H2A.Z and DNA methylation are mutually antagonistic chromatin marks. *Nature* **456**, 125-129.

FIGURE LEGENDS

Figure 1. Physical interactions between SWC4 and SWC6.

(A) SWR1-C related proteins co-purified with SWC6. Number of peptides identified by mass spectrometry after immunoprecipitation in samples eluted (E) with c-Myc peptide or that remain in the agarose beads (B), from SWC6-myc and negative control seedlings.

(B) Y2H assays showing that SWC6 interacts with SWC4. Full-length SWC6 and SWC4 proteins were fused to the GAL4-Activation and DNA binding domain, respectively. Yeast transformed with these constructs or empty vectors were grown with increasing concentrations of 3-AT (0, 15mM and 25 mM). Three-fold decreasing dilutions of yeast were plated left to right in each panel.

(C) Co-IP assays in agroinfiltrated *N. benthamiana* plants. SWC4-GFP, GFP-SWC4 and Myc-SWC6 fusion proteins were produced alone or in combination in wild *Nicotiana* plants, and GFP fusion proteins were immunoprecipitated with GFP-Trap_A (ChromoTek) and Myc-SWC6 was detected using anti c-Myc (Millipore, clone 4A6).

Figure 2. Disruption of the SWC4 gene affects embryo development whereas Knockdown expression of SWC4 mRNA results in pleiotropic developmental abnormalities.

(A) Schematic representation of *swc4-1* T-DNA insertion.

(B) Number of normal and abnormal seeds in heterozygous *swc4-1/+* siliques. Error bars indicate \pm sd.

(C) Open silique of a *swc4-1/+* plant. Arrows indicate the abnormal seeds formed.

(D) Picture of embryos from Col seeds and *swc4-1/+* white seeds containing arrested abnormal embryos. Scale bar = 70 μ m .

(E) Distribution of aborted seeds in heterozygous *swc4-1/+* siliques. The silique from heterozygous *swc4-1/+* plants was divided into 25 regions to quantify the

distribution of abnormal seeds. The majority of aborted seeds were localized in the region close to the stigma and only a minor fraction at the bottom of the silique.

(F) Q-PCR analysis of the expression of *SWC4* in 16 day-old RNAi line 712 (*swc4i*) seedlings grown under SD conditions. Error bars indicate \pm sd (n=3).

(G) Col and *swc4i* plants grown under LD and SD for 3 and 9 weeks, respectively.

(H) Rosette leaves of Col and *swc4i* plants grown under LD conditions.

(I) Pictures showing the organ size reduction in *swc4i* compared to Col. Detail of flowers, petals, stamens, carpels and siliques size from Col (left) and *swc4i* (right) plants grown under SD conditions.

Figure 3. SWC4 regulates leaf cell proliferation and expansion processes.

(A) Rosette diameter of 32 day-old Col and *swc4i* plants grown under LD and SD conditions (n=10). Error bars indicate \pm sd; *** $p < 0.001$ (Student's t-test).

(B) Average leaf blade size (mm²) of leaves 3 and 4 from 32 day-old Col and *swc4i* plants grown under SD conditions (n=20). Error bars indicate \pm sd; *** $p < 0.001$ (Student's t-test).

(C) SEM images of adaxial leaf epidermal layers of Col and *swc4i* plants (200x). Scale bar = 50 μ m.

(D-F) Cell number per unit area **(D)**, cell size distribution **(E)** and estimated cell area **(F)** in the adaxial leaf epidermis of Col and *swc4i* plants. Measurements were carried out in the central region of at least seven leaves. (n \geq 200 cells). Error bars indicate \pm sd; *** $p < 0.001$ (Student's t-test).

(G-H) Nuclear DNA ploidy distribution in Col and *swc4i* plants grown under SD **(G)** and LD **(H)** conditions. The results shown are the average of three independent assays. Error bars indicate \pm sd.

Figure 4. SWC4 knockdown alters the expression of flowering time genes.

(A-B) Total leaf number of Col, *swc6-1* and *swc4i* plants grown under LD **(A)** and SD **(B)** conditions. In SD conditions about 40% of the *swc4i* plants grown did not flower and were not included in the graph calculations. Flowering time data are the average of 30 plants. Error bars indicate \pm sd; * $p < 0.05$, *** $p < 0.001$ (Student's t-test).

(C-H) Q-PCR expression analysis of flowering time genes (*FT*, *SOC1* and *FLC*) over a 24h time course in Col, *swc6-1* and *swc4i* seedlings grown for 11 days in LD **(C,E, G)** and 19 days in SD **(D,F,H)** conditions. Samples were harvested every 4 h after dawn. ZT means Zeitgeber time. The data represent the average of 3 biological replicates and error bars indicate \pm sd.

Figure 5. SWC4 modulates H2A.Z deposition.

(A) Pie chart showing the distribution of annotated HTA9 peaks in Col seedlings relative to nearby genomic features including TSS, exons, introns and untranslated regions.

(B) Metagene plot of ChIP-seq z-score-normalized HTA9 values across all genes -/+ 2 kb in Col and *swc4i*.

(C) Heatmap showing the distribution of Col and *swc4i* HTA9 levels in a 1kb region upstream and downstream of the TSS across all *Arabidopsis* genes. Each row represents the normalized ChIP-seq \log_2 HTA9/Input ratio over one gene.

(D) Box-plot of z-score normalized HTA9 ChIP-seq levels in differentially enriched HTA9 regions in Col and *swc4i* (* $p < 2.2 \times 10^{-15}$, Wilcoxon rank-sum test).

(E) Venn diagram showing the overlap between downregulated genes with low H2A.Z levels in *swc4i* compared to Col.

(F) Venn diagram showing the overlap between upregulated genes with low H2A.Z levels in *swc4i* compared to Col (*** hypergeometric test $p < 0.001$).

Figure 6. *Arabidopsis* SWC4 is a DNA-binding protein that preferentially recognizes AT-rich DNA elements.

(A) Position weight matrix representation of the DNA motifs obtained for SWC4 in protein binding microarray assay.

(B) AT-rich DNA binding elements are enriched around TSS of SWC4-target genes. Plot represents the density of SWC4 binding sequences around the TSS (position 0, x-axis), covering 0.5 kb upstream and downstream of the TSS, and include average densities for all the *Arabidopsis* genes contained in The Arabidopsis Information Resource database (TAIR10, blue line) and the subgroup of genes upregulated and with low H2A.Z levels in *swc4i* (red line).

Figure 7. SWC4 binds defined AT-rich DNA elements to recruit SWR1-C at *FT* chromatin.

(A) Schematic representation of *FT* locus indicating the regions analyzed by ChIP. Arrows indicate AT-rich DNA elements at *FT* chromatin (Supplemental Data S5).

(B-C) ChIP experiments using α -HTA9 **(B)** and α -H4K5ac **(C)** in WT and *swc4i* seedlings. Data are represented as the fraction of immunoprecipitated DNA normalized to an *ACTIN* gene region. Graphs represent the average of 3 independent biological ChIP experiments quantified by Q-PCR. Error bars indicate \pm sd (***) $p < 0.001$; Student's t-test).

(D) ChIP experiments using α -SWC4 antibody in WT seedlings. No Ab means mock immunoprecipitation sample without antibody. Data are the average of 3 independent biological ChIP experiments quantified by Q-PCR and is represented as %INPUT. Error bars indicate \pm sd.

Figure 8. SWC4 mediates the recruitment of SWR1-C to the chromatin of key regulatory transcription factors by recognizing AT-rich DNA elements.

(A) ChIP experiments using α -SWC4 antibody in WT seedlings showing the binding of SWC4 at *FT*, *FUL*, *IAA19* and *ERF9* loci. Data are the average of 3 independent biological ChIP experiments quantified by Q-PCR and is represented as %INPUT. Error bars indicate \pm sd.

(B-D) H2A.Z ChIP-seq data of *FUL* (B), *IAA19* (C) and *ERF9* (D) displayed using the Integrative Genomics Viewer (IGV, Broad Institute) showing a schematic representation of the gene, WT (blue) and *swc4i* (red) HTA9 z-score values. SWC4 ChIP-binding sites (red line) localize over H2A.Z peaks and encompass AT-rich DNA elements (arrows) identified using matrix-scan RSAT tool (Markov order 1; $p < 0.01$).

(E) Working model for the role of SWC4 in the SWR1-C-mediated deposition of H2A.Z at target loci.

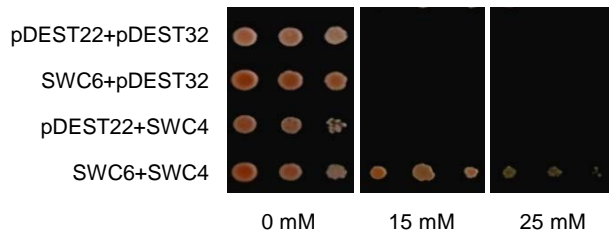
SWR1-C catalyzes ATP-dependent deposition of H2A.Z, but the recruitment mechanism of SWR1-C to promoter regions remains unclear. In all eukaryotes analyzed, NFR are flanked by H2A.Z-containing nucleosomes around the TSS. SWR1-C might preferentially bind to long nucleosome-free AT-rich DNA, allowing discrimination of gene promoters over gene bodies. In *Arabidopsis* H2A.Z is preferentially located in TSS but lacks upstream H2A.Z nucleosomes and H2A.Z occupancy at nucleosome +1 is inversely correlated with gene expression levels. Our data show that *Arabidopsis* SWC4 binds DNA, recognizing preferentially AT-rich DNA elements that are over-represented in the promoters of a subset of genes where H2A.Z incorporation impairs transcription. H2A.Z –containing nucleosomes are depicted as orange square whereas white square correspond to H2A-containing nucleosomes.

Figure 1

A

Protein	Name	Experiment No.1				Experiment No.2			
		SWC6-myc		Control		SWC6-myc		Control	
		E	B	E	B	E	B	E	B
Q8LGE3	ARP6	16	6	0	0	14	6	0	0
Q8VZL6	SWC4	2	0	0	0	1	0	0	0
Q9FH40	YAF9A	1	0	0	0	0	0	0	0
Q0WT50	SWC2	0	0	0	0	0	1	0	0
Q7X9V2	PIE1	1	0	1	0	3	1	1	0
Q9FJW0	RVB2A	6	15	0	2	0	0	0	0
Q9M2X5	RVB2B	1	1	0	0	0	0	0	0
Q9FMR9	RVB1	10	15	4	8	1	1	0	0
Q84M92	ARP4	26	34	12	18	45	1	24	0

B



C

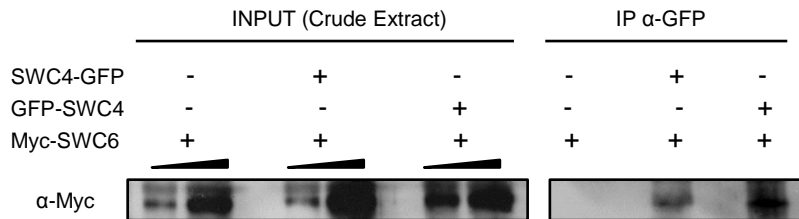


Figure 2

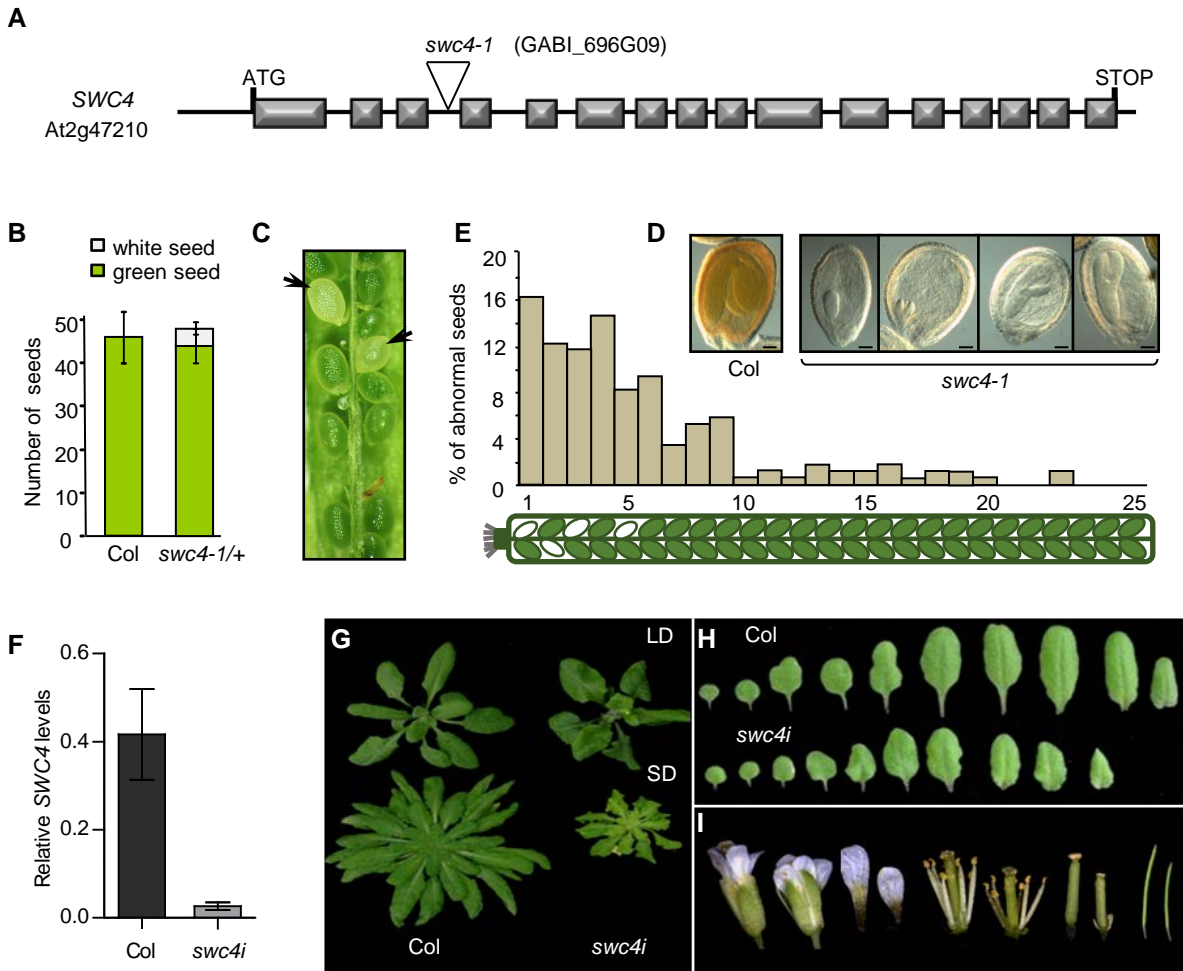


Figure 3

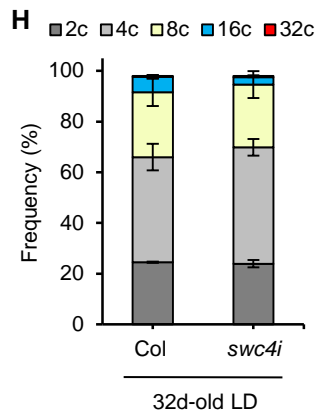
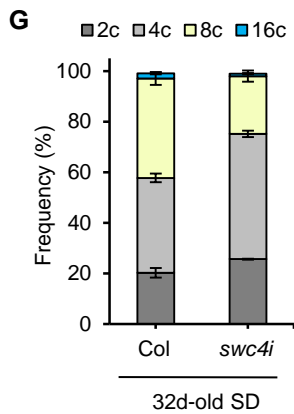
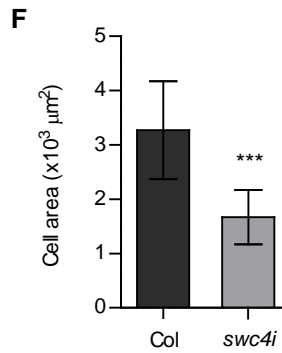
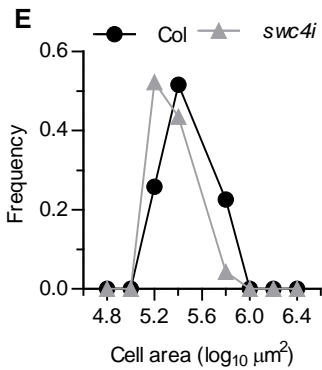
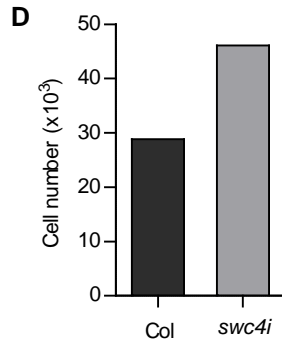
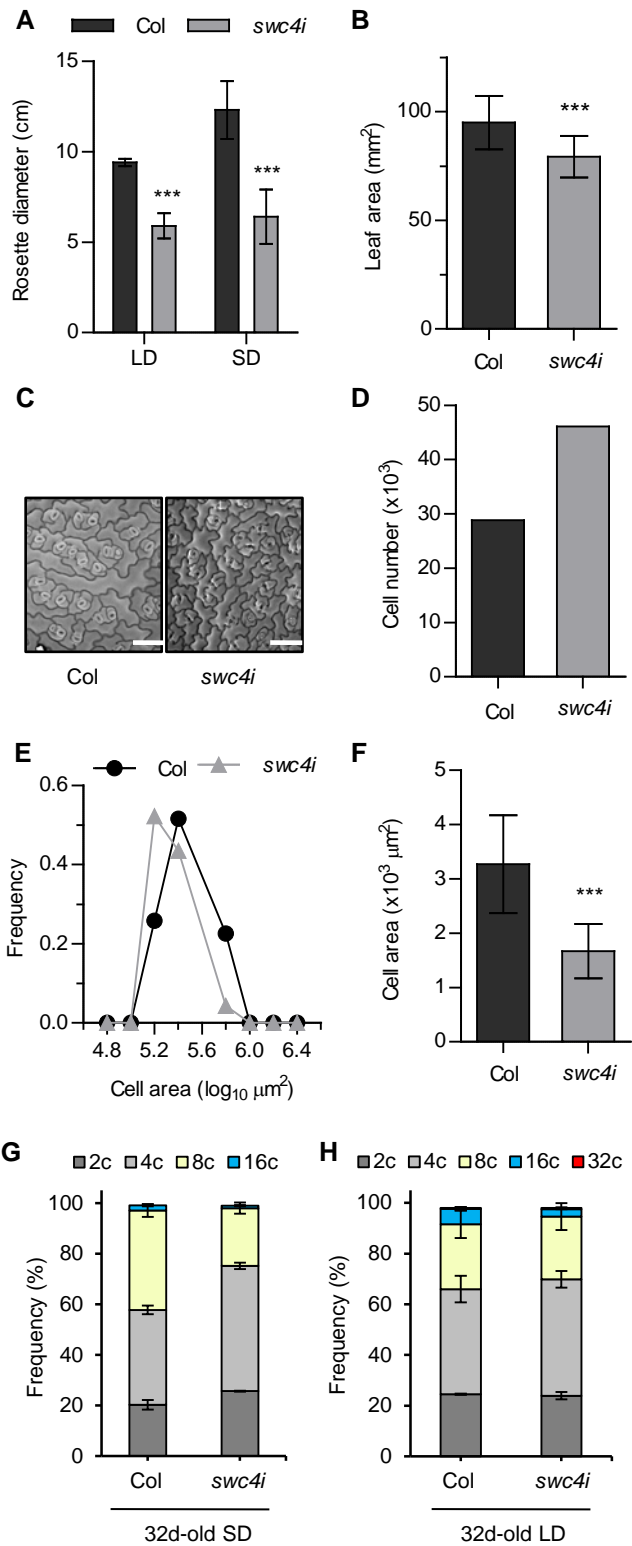


Figure 4

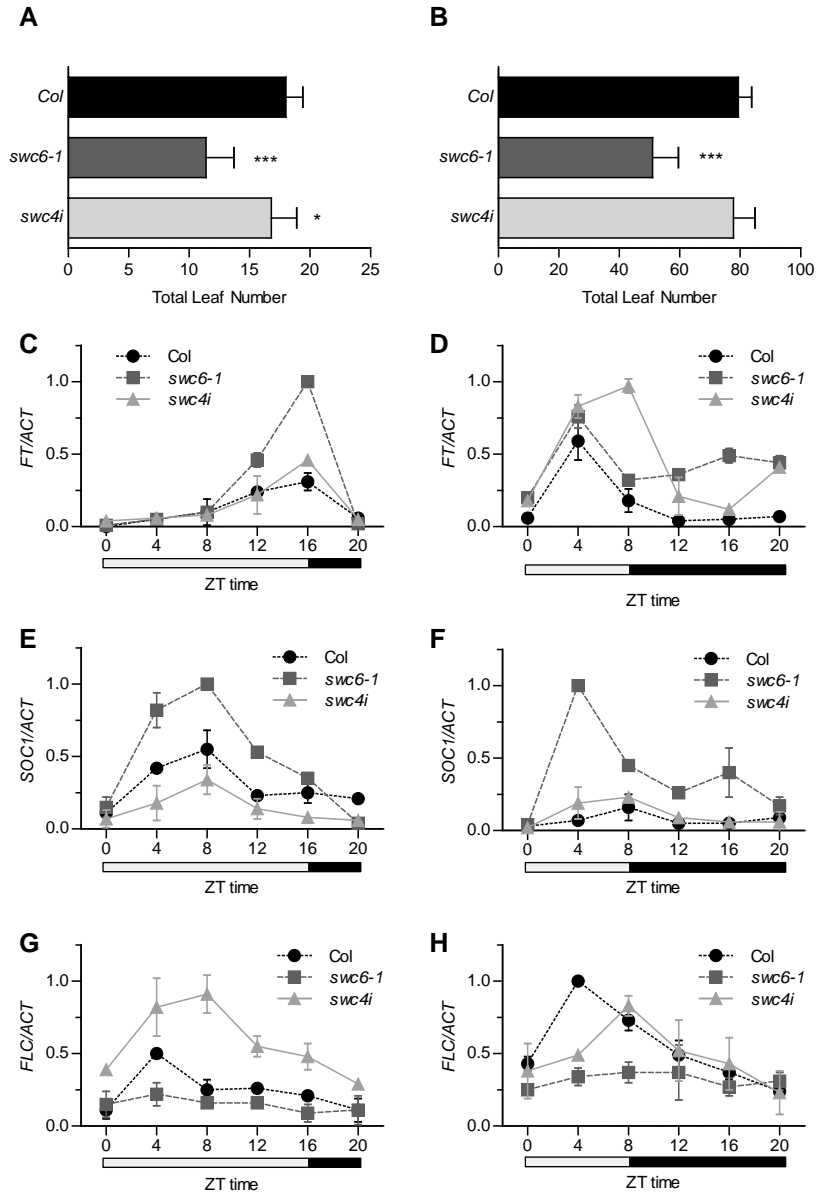


Figure 5

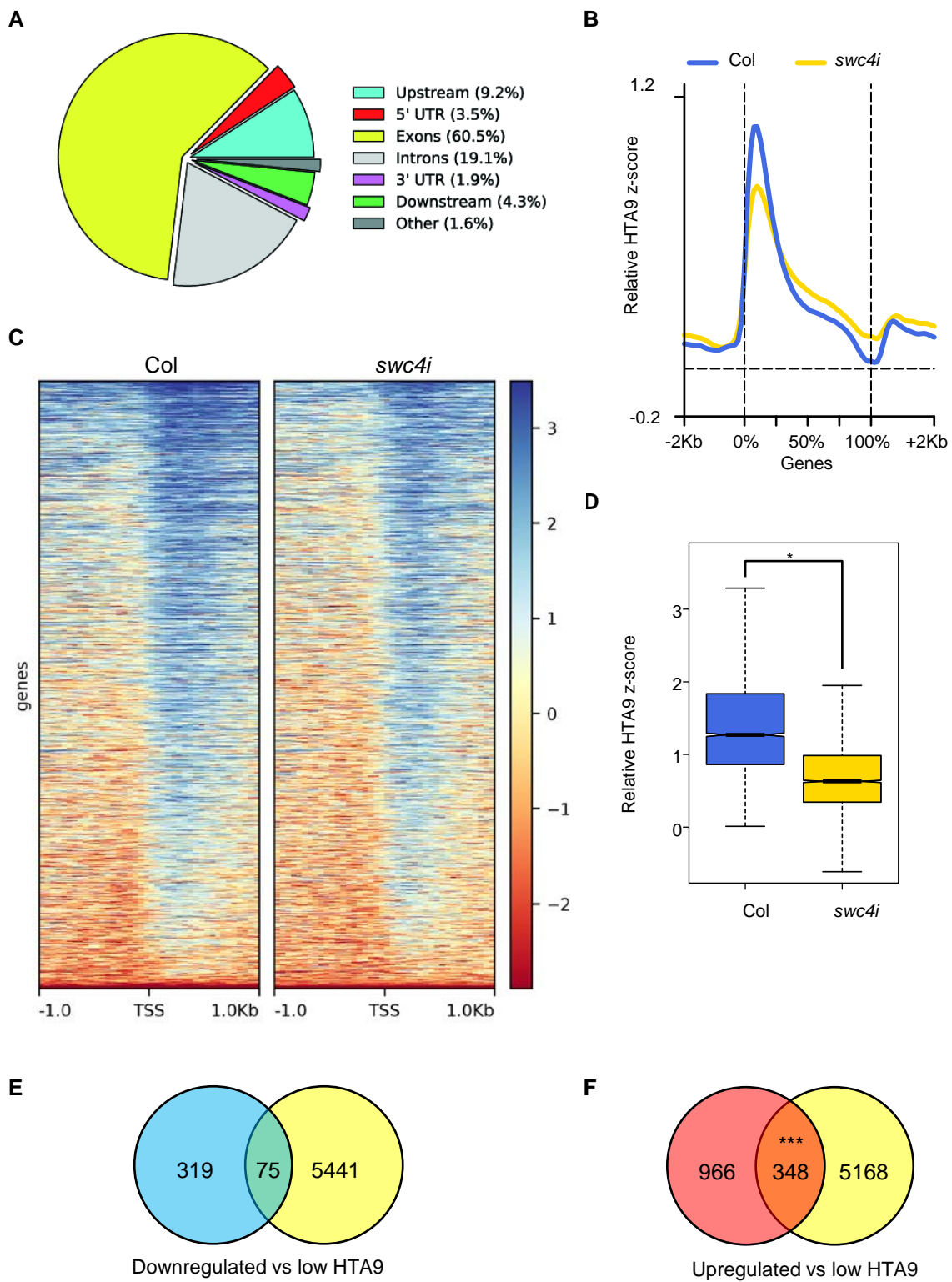








Figure 6

A

Sequence logo	8-mer	E-score	Z-score
	AATTAAAT	0.45052	5.6179
	AAATAAAA	0.44536	5.6031
	AATATAAA	0.44460	5.2329
	TTAATTAA	0.44285	5.6122
	AATTTAAT	0.44122	5.0928
	AATAAATA	0.44055	4.8081

B

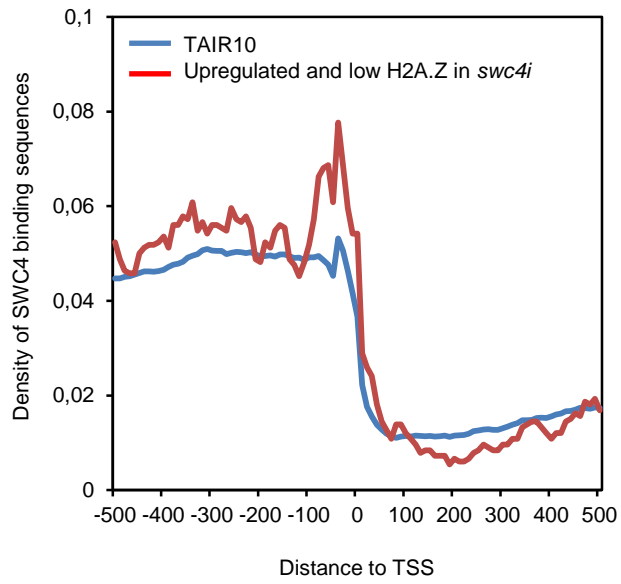


Figure 7

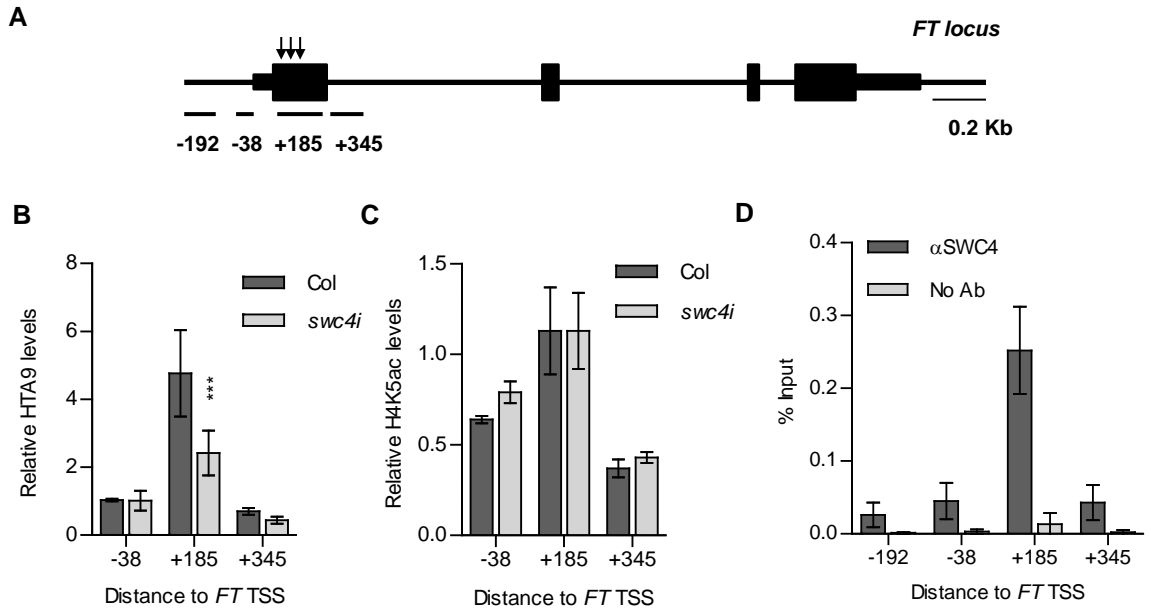


Figure 8

